

VARIABLE STARS IN THE GLOBULAR CLUSTER NGC 2808

ANDREA KUNDER¹, PETER B. STETSON², MÁRCIO CATELAN^{3,4}, ALISTAIR R. WALKER¹, AND PÍA AMIGO^{3,4}

¹ Cerro Tololo Inter-American Observatory, Casilla 603, La Serena, Chile; akunder@ctio.noao.edu

² Dominion Astrophysical Observatory, Herzberg Institute of Astrophysics, National Research Council, Victoria, BC, Canada

³ Departamento de Astronomía y Astrofísica, Pontificia Universidad Católica de Chile, Av. Vicuña Mackenna 4860,

782-0436 Macul, Santiago, Chile; mcatelan@astro.puc.cl

⁴ The Milky Way Millennium Nucleus, Av. Vicuña Mackenna 4860, 782-0436 Macul, Santiago, Chile

Received 2012 September 26; accepted 2012 November 16; published 2013 January 2

ABSTRACT

The first calibrated broadband *BVI* time-series photometry is presented for the variable stars in NGC 2808, with observations spanning a range of 28 years. We have also redetermined the variability types and periods for the variable stars identified previously by Corwin et al., revising the number of probable fundamental-mode RR Lyrae variables (RR0) to 11 and the number of first-overtone variables (RR1) to five. Our observations were insufficient to discern the nature of the previously identified RR1 star, V24, and the tentatively identified RR1 star, V13. These two variables are ~ 0.8 mag brighter than the RR Lyrae variables, appear to have somewhat erratic period and/or luminosity changes, and lie inside the RR Lyrae instability strip. Curiously, all but one of the RR Lyrae stars studied in this relatively metal-rich cluster exhibit the Blazhko phenomenon, an effect thought to occur with higher frequency in metal-poor environments. The mean periods of the RR0 and RR1 variables are $\langle P \rangle_{RR0} = 0.56 \pm 0.01$ d and $\langle P \rangle_{RR1} = 0.30 \pm 0.02$ d, respectively, supporting an Oosterhoff I classification of the cluster. On the other hand, the number ratio of RR1-to-RR0-type variables is high, though not unprecedented, for an Oosterhoff I cluster. The RR Lyrae variables have no period shifts at a given amplitude compared to the M3 variables, making it unlikely that these variables are He enhanced. Using the recent recalibration of the RR Lyrae luminosity scale by Catelan & Cortés, a mean distance modulus of $(m - M)_V = 15.57 \pm 0.13$ mag for NGC 2808 is obtained, in good agreement with that determined here from its type II Cepheid and SX Phoenicis population. Our data have also allowed the discovery of two new candidate SX Phoenicis stars and an eclipsing binary in the blue straggler region of the NGC 2808 color-magnitude diagram.

Key words: globular clusters: individual (NGC 2808) – stars: distances – stars: horizontal-branch – stars: Population II – stars: variables: general – stars: variables: RR Lyrae

Online-only material: color figures

1. INTRODUCTION

NGC 2808 is one of the most luminous globular clusters (GCs) in the Galaxy ($M_V = -9.39$) and also one of the most magnificent, especially in terms of its color-magnitude diagram (CMD). Not only is its main sequence (MS) a fusion of three distinct sequences interpreted as successive episodes of star formation (D'Antona et al. 2005; Piotto et al. 2007), but its horizontal branch (HB) is multimodal with a greatly extended hot blue tail that covers a range of ~ 5 mag, in V , below the mean level of the instability strip (IS) (Bedin et al. 2000; Dalessandro et al. 2011). A multimodal HB is not easily explained; GCs with red HB stars cooler than the RR Lyrae gap are generally associated with relatively high metallicities, while those with blue HB stars tend to be metal-poor systems. However, multimodal HBs do not fit into this common paradigm, and therefore such clusters may help to provide a key to more general understanding of the HBs of GCs (e.g., Catelan et al. 1998a; Catelan 2008, 2009, and references therein).

The three MS branches in NGC 2808 are thought to be associated with structures in its HB: it has been put forth by D'Antona et al. (2005) that the three MS populations all have different helium abundances leading to three different HB populations. According to their models, the RR Lyrae variables (RRLs) could be either the bluest extension of the red clump population, which has a normal He, or they could be the reddest part of the blue clump, which contains stars that are slightly helium enhanced ($0.26 < Y < 0.29$). Although the existence

of the high-helium ($Y \sim 0.40$) population as well as the normal-helium population seems robust (D'Antona et al. 2005; Bragaglia et al. 2010; Pasquini et al. 2011), the intermediate-helium population is inferred only from the HB morphology. In this sense, the RRLs are particularly valuable as potential support for the existence of the intermediate-helium population. Similarly, models from Lee et al. (2005) and Dalessandro et al. (2011) predict normal He for the red HB, and enhanced He for the blue HB, but by and large do not discuss the IS.

Here, an observational analysis of one of the HB components in NGC 2808, the RR Lyrae IS, is presented. This component is largely unexplored, especially because RRLs were not even thought to be a major constituent of NGC 2808 until Corwin et al. (2004) discovered a number of these variables, raising the number of candidate RRLs to 18. The Corwin et al. (2004) variables are all located in its crowded core, so placing the light curves on a photometrically calibrated scale was not then possible.

However, investigating the helium enhancement of RR Lyrae variables requires knowledge of their luminosities (e.g., Asano & Sugimoto 1968; van Albada & Baker 1971; Sweigart et al. 1987; Cáceres & Catelan 2008; Dalessandro et al. 2011). This is because their mean luminosity is a function of He. Calibrated amplitudes are also important because these are correlated to their T_{eff} , which in turn can be compared to their period to understand potential “period shifts” (e.g., Carney et al. 1992; Catelan 1998; De Santis 2001). The period shift is usually made between the RRLs in different globular clusters (Sandage 1981,

Table 1
NGC 2808 Observations

Run ID	Dates	Telescope/Camera/Detector	<i>U</i>	<i>B</i>	<i>V</i>	<i>R</i>	<i>I</i>	Note
1 ct83	1983 Feb 12	CTIO 4.0m RCA	...	2	2	
2 ct84	1984 Mar 7	CTIO 4.0m RCA	...	1	1	
3 ct85	1985 Apr 18	CTIO 4.0m RCA	...	1	1	
4 pab	1987 Jan 23–24	CTIO 0.9m RCA	...	12	12	
5 aat	1991 Jan 13	AAT 3.9m CCD_1	...	6	...	15	...	
6 emmi3	1994 Dec 26	ESO NTT 3.6m EMMI TK2048EB	4	...	3	
7 emmi2	1995 Mar 8–10	ESO NTT 3.6m EMMI TK2048EB	18	...	19	
8 zingle	1996 Apr 16–19	CTIO 0.9m Tek2K_3	18	...	16	
9 apr97	1997 Apr 12	ESO Dutch 0.91m Tektronix 33	6	...	6	
10 bond5	1997 Jun 2	CTIO 0.9m Tek2K_3	2	2	2	...	2	
11 bond3	1997 Nov 9–11	CTIO 0.9m Tek2K_3	3	3	3	...	3	
12 dec97	1997 Dec 26–27	ESO Dutch 0.91m Tektronix 33	14	...	14	
13 roddy	1998 Jan 26–28	ESO Danish 1.54m DFOSC Loral	6	20	17	...	10	
14 bond6	1998 Apr 17–19	CTIO 0.9m Tek2K_3	2	2	2	...	2	
15 bond4	1999 Jun 13–16	CTIO 0.9m Tek2K_3	4	2	2	...	2	
16 wfi11	1999 Dec 6–7	ESO MP 2.2m WFI	8	10	9	a
17 bond7	2001 Mar 25	CTIO 0.9m Tek2K_3	1	1	1	...	1	
18 wfi6	2002 Feb 19–21	ESO 2.2m MP WFI	...	4	4	...	6	a
19 dan0210	2002 Oct 15–16	ESO Danish 1.54m DFOSC MAT/EEV	36	
20 dan0212	2002 Dec 12–15	ESO Danish 1.54m DFOSC MAT/EEV	...	76	72	
21 dan0302	2003 Feb 19–20	ESO Danish 1.54m DFOSC MAT/EEV	...	83	81	
22 emmi0305	2003 May 10–11	ESO NTT 3.6m EMMI emred	74	
23 fors3	2005 Feb 16–17	ESO VLT 8.0m FORS2	...	13	19	b
24 dan0504	2005 Apr 29	ESO Danish 1.54m DFOSC EEV	...	23	21	
25 dan0505	2005 May 12–13	ESO Danish 1.54m DFOSC EEV	...	32	33	
26 fors20605	2006 May 29	ESO VLT 8.0m FORS2 ccdf	1	3	1	b
27 soar0906	2009 Feb 27	SOAR 4.1m SOI	10	9	9	...	13	b
28 efosc0904	2009 Apr 16	ESO NTT 3.6m EFOSC LORAL	...	240	
29 efosc09	2009 Apr 19–26	ESO NTT 3.6m EFOSC LORAL	...	68	7	
30 pia	2010 Jan 10–15	CTIO 1.0m Y4KCam	...	15	15	...	15	
31 soar10a	2010 Jan 14	SOAR 4.1m SOI	3	5	6	...	4	b
32 soar10bc	2010 Jan 20–21	SOAR 4.1m SOI	11	11	7	...	9	b
33 soar10d	2010 Feb 8	SOAR 4.1m SOI	7	7	7	...	14	b
34 soar10j	2010 Oct 14	SOAR 4.1m SOI	...	30	30	...	28	b
35 andrea1	2010 Apr 27–28	CTIO 1.0m Y4KCam	18	17	...	
36 andrea2	2010 Jun 27	CTIO 1.0m Y4KCam	4	3	...	
37 Y1101	2011 Jan 13–18	CTIO 1.0m Y4KCam	...	46	73	66	50	
38 Y1104	2011 Apr 14–18	CTIO 1.0m Y4KCam	69	1	57	

Notes. 1. Observers J. Hesser & R. McClure. 2. Observers J. Hesser & R. McClure. 3. Observers J. Hesser & R. McClure. 4. Observer P. Bergbusch. 5. Observers Da Costa & Norris. 6. Observer Testa, Project ID 054.E-0404. 7. Observer Zaggia, Project ID 054.E-0337. 8. Observer R. Zingle. 9. Observer A. Rosenberg. 10. Observer H. E. Bond. 11. Observer H. E. Bond. 12. Observer A. Rosenberg. 13. PI L. Bedin. 14. Observer H. E. Bond. 15. Observer H. E. Bond. 16. Observer A. Recio Blanco, Program ID 064.L-0255. 17. Observer H. E. Bond. 18. Program ID 68.D-0265(A). 19. Observer T. M. Corwin, M. Catelan, & J. M. Fernández, Program ID 02/8232. 20. Observer J. Borissova & M. Catelan, Program ID 02/8232. 21. Observer T. M. Corwin, M. Catelan, Program ID 02/8232. 22. Program ID 071.D-0609(A). 23. Program ID 074.D-0187(B). 24. Observer R. Salinas. 25. Observer R. Salinas. 26. Program ID 077.D-0775(A). 27. Observer M. Smith, Proposal ID 2008B-0482. 28. Program ID 083.D-0833(A). 29. Program ID 083.D-0544(A). 30. Observers C. Gatica & A. Brito. 31. Observer “MSU,” Proposal ID 2009B-0340. 32. Proposal ID 2009A-0414. 33. Observer Smith, Proposal ID 2010A-0312. 34. Observers S. Zepf & M. Peacock. 35. Observers A. Kunder, J. Subasavage & J. Seron. 36. Observer A. Kunder. 37. Observers A. Kunder & S. A. Stubbs. 38. Observer A. Kunder.

^a Eight individual CCD chips in the camera; the reported number of CCD images is the number of exposures × 8.

^b Two individual CCD chips in the camera.

1993; Sandage et al. 1981; Carney et al. 1992) and can be used as an indicator for [Fe/H], luminosity, or Oosterhoff (Oo) type (e.g., Cacciari et al. 2005). In particular, if the enhancement of He is present in the RRLs, large period shifts are clearly expected (see, e.g., Sweigart et al. 1987; Catelan et al. 1998b; Marconi et al. 2011; Kunder et al. 2012).

In this paper, new and archival *BVI* photometry of NGC 2808 is presented, which has allowed the first calibrated light curves of the RR Lyrae variables. The discovery of additional variable stars and the re-examination of the currently known variables in the cluster are also reported. Constraints on the cluster’s formation history from the ancient RRLs are put forward.

2. OBSERVATIONS

The observational material for this study consists of 2475 individual CCD images from 38 observing runs. These images are contained within a data archive maintained by author P.B.S., and include—among others—the images employed by Corwin et al. (2004), as well as some images obtained specifically for this project: five nights of observations in 2010 January, two nights in 2010 April, and four nights in 2011 January, all carried out on the SMARTS 1 m telescope at Cerro Tololo. The summary details of all 38 observing runs are given in Table 1. Considering all these images together, the median seeing for our

observations was $1''.09$; the 25th and 75th percentiles were $0''.88$ and $1''.35$; the 10th and 90th percentiles were $0''.74$ and $1''.69$.

The photometric reductions were all carried out using standard DAOPHOT/ALLFRAME procedures (Stetson 1987, 1994) to perform profile-fitting photometry, which was then referred to a system of synthetic-aperture photometry by the method of growth-curve analysis (Stetson 1990). Calibration of these instrumental data to the photometric system of Landolt (1992; see also Landolt 1973, 1983) was carried out as described by Stetson (2000, 2005). If we define a “data set” as the accumulated observations from one CCD chip on one night with photometric observing conditions, or one chip on one or more consecutive nights with non-photometric conditions, the data for NGC 2808 were contained within 90 different data sets, each of which was individually calibrated to the Landolt system. Of these 90 data sets, 61 were obtained and calibrated as “photometric,” meaning that photometric zero points, color transformations, and extinction corrections were derived from all standard fields observed during the course of that night, and applied to the NGC 2808 observations. The other 29 data sets were reduced as “non-photometric;” in this case, color transformations were derived from all the standard fields observed, but the photometric zero point of each individual CCD image of NGC 2808 was derived from local photometric standards contained within the image itself.

The different cameras employed projected to different areas on the sky, and, of course, the telescope pointings differed among the various exposures. The EMMI MIT/LL, FORS, SOI, and WFI imagers, in particular, consist of mosaicks of non-overlapping CCD detectors. Therefore, although we have 2475 images, no individual star appears clearly in all those images. In fact, no star appeared in more than 73 U -band images, 672 B images, 564 V images, or 267 I images. The median number of observations for one of our stars is 16 in U , 143 in B , 248 in V , and 147 in I . Since most pointings were centered on or near the cluster, member stars typically have more observations than field stars lying far from the cluster center.

There were insufficient R -band images to define local standards in the NGC 2808 field, so we have not calibrated the R data. Furthermore, during the “dan0210” observing run (number 19 in Table 1) there were some 38 images apparently obtained in a long-wavelength band, most likely the Z band; they were incorrectly identified as “bessell B ” in the FITS image headers, but from the magnitude differences observed between red/blue pairs of stars, the filter evidently had a longer effective wavelength than I . These Z - and R -band images were included in the ALLFRAME analysis for the additional information that they give on the completeness of the star list and the precision of the astrometry, but we make no further use of them here.

It should also be noted that calibration of U -band data is notoriously problematic because significantly different prescriptions for the U filter are employed in different filter sets, the quantum efficiency of many CCDs is highly wavelength dependent within the U bandpass, and the form of the bandpass itself is further modified by the wavelength-dependent transparency of the terrestrial atmosphere. Thus, while we have obtained U -band photometry for NGC 2808 and have calibrated it to the Landolt system to the best of our ability, we do not employ it here for any scientifically critical inferences.

The astrometric calibration is tied to the U.S. Naval Observatory (USNO) A2.0 Astrometric Reference Catalog. Positions of stars encompassing our target field were downloaded from the USNO interface of the Canadian Astronomy Data Centre

(CADC). From the CADC we also downloaded all available images of our field from the Digitized Sky Survey; in the case of NGC 2808, scans of five plates were available: one IIIaJ+GG395 ($\sim B$), one IIaD+GG495 ($\sim V$), two IIIaF+OG590 ($\sim R$), and one IVN+RG715 ($\sim I$). Positions and magnitude indices of star-like objects in the digitized photographic images were obtained using the software of Stetson (1979). These positions were referred to the coordinate system of the USNO A2.0 catalog, employing 20 constant cubic polynomial transformations based on 10,000–22,000 stars per plate, and averaged. Then the positions of stars in the CCD images were all transformed to this average coordinate system via cubic polynomials and averaged. We find that, compared to the weighted average of all measured positions, the USNO A2.0 catalog has rms positional residuals of $0''.22$ in each coordinate; each of the five digitized plates had rms residuals ranging from $0''.16$ to $0''.23$; and the CCD positions had rms residuals of $0''.06$. Since these transformations were based on more than 20,000 stars, we believe that it is safe to say that our positions are on the USNO A2.0 astrometric system to within well under $0''.1$. If the USNO system itself contains systematic errors larger than this relative to some other “true” astrometric system, then our positions have inherited those systematic errors. We believe that within that overall system, our relative star-to-star positions are internally precise to better than $0''.03$, depending, of course, on the signal-to-noise ratio of the individual stellar detections.

3. VARIABLE STARS IN NGC 2808

Several authors have reported variable stars in NGC 2808. The first finding chart of seven variables was published by Fourcade & Laborde (1966), although five of these are now thought to be actually non-varying (Clement & Hazen 1989). Alcaino (1971) identified two further variables, which were also later determined to be non-varying (Clement & Hazen 1989). The study by Clement & Hazen (1989) produced three new variables, bringing the number of confirmed variables to five. With the advent of modern CCD observations and data reduction techniques, Corwin et al. (2004) announced 18 new variables close to the crowded cluster core. Unfortunately, because of the compact nature of this cluster, they were unable to place the light curves on a photometrically calibrated scale. The first candidate variable stars using the *Hubble Space Telescope* (*HST*) were found by Dieball et al. (2005). As the *HST* observations were taken over four days only, reliable light curves and periods for the six variable candidates were not obtained. One of their candidates corresponds with V22, an RRL identified by Corwin et al. (2004), and the rest of their candidates are considerably fainter. Long-period variables (LPVs) were searched for by Lebzelter & Wood (2011), resulting in the determination of periods and amplitudes for 15 LPVs.

Besides the LPVs, no calibrated CCD time-series photometry has been presented for any of the confirmed variables in NGC 2808. The time-series observations presented here cover a baseline that allows for the potential to detect variability on timescales from hours to months. Therefore, we are in a position to re-examine and revise the list of variables in the cluster.

The characteristics of the confirmed variables are given in Table 2. Although seven previously identified variables were too blended to derive reliable calibrated magnitudes and amplitudes, we were able to obtain periods for these stars from their instrumental light curves. The positions of all the variables, as well as for the constant stars (NV) that have been incorrectly identified as variables by others, are also listed for completeness.

Table 2
Variable Stars Detected in NGC 2808

Name	R.A. (J2000.0)	Decl. (J2000.0)	Period (days)	(B) _{mag}	(V) _{mag}	(I) _{mag}	$\langle B \rangle$	$\langle V \rangle$	$\langle I \rangle$	A_B	A_V	A_I	Type	Comment	
V1	09 12 20.22	-64 52 20.5	...	14.8	13.4	11.2	LPV	
V2	09 11 55.66	-64 51 10.5	...	15.92	14.64	13.23	NV	
V3	09 12 08.38	-64 51 47.3	...	16.83	15.82	14.64	NV?	large W/S index, poss. $P = 80$ d
V4	09 11 33.77	-64 51 43.8	...	19.00	18.09	16.96	NV	
V5	09 12 09.57	-64 51 52.4	...	16.62	16.49	16.25	NV	
V6	09 12 30.08	-64 56 37.9	0.538968	16.75	16.31	15.62	16.74	16.29	15.60	1.08	0.75	0.71	RR0	Blazhko	
V7	09 13 13.13	-64 50 46.5	...	15.16	13.54	11.82	NV	
V8	09 12 06.56	-64 53 49.3	...	15.83	14.76	13.50	NV	
V9	09 11 53.06	-64 54 24.3	...	16.82	16.24	15.41	NV	
V10	09 11 56.86	-64 53 23.2	1.76528	15.92	15.30	14.48	15.91	15.28	14.47	1.02	0.73	0.47	BL Her		
V11	09 12 06.72	-64 52 40.3	...	14.5	12.9	11.1	LPV	
V12	09 11 56.15	-64 50 09.6	0.305776	16.62	16.26	15.72	16.63	16.27	15.71	0.58	0.45	0.28	RR1	Blazhko	
V13	09 12 23.35	-64 57 10.6	0.173678	16.09	15.52	14.76	16.26	15.59	14.79	0.18	0.18	0.16	W UMa?	ellipsoidal binary?	
V14	09 12 13.40	-64 51 04.0	0.598903	16.75	16.27	15.53	16.76	16.26	15.53	0.98	0.73	0.45	RR0	field star	
V15	09 12 10.61	-64 51 15.7	0.610975	16.82	16.31	15.46	16.84	16.29	15.46	0.46	0.38	0.23	RR0	Blazhko	
V16	09 12 09.11	-64 52 51.5	0.605218	16.75	16.32	15.67	16.74	16.29	15.68	0.70	0.66	0.46	RR0	Blazhko	
V17	09 12 07.01	-64 51 57.3	0.504050::	RR0?	blend	
V18	09 12 06.57	-64 52 17.0	0.5851455	RR0	Blazhko, slightly blended	
V19	09 12 06.26	-64 52 10.7	0.5091927::	RR0	blend	
V20	09 12 05.32	-64 51 26.5	0.287021	16.55	16.01	15.37	16.55	16.04	15.37	0.69	0.43	0.29	RR1	Blazhko	
V21	09 12 03.90	-64 51 25.9	0.604334	RR0	blend	
V22	09 12 03.87	-64 51 55.3	0.518688	RR0	blend	
V23	09 12 03.26	-64 52 19.7	0.265985	16.51	16.05	15.47	16.50	16.08	15.47	0.56	0.34	0.16	RR1	Blazhko	
V24	09 12 02.62	-64 52 10.7	0.268199::	16.12	15.55	14.74	16.18	15.66	14.83	0.54	0.24	0.19	W UMa?	properties uncertain	
V25	09 11 58.68	-64 51 27.9	0.49517::	RR0	blend	
V26	09 11 53.09	-64 51 30.7	0.365099	16.48	16.16	15.63	16.47	16.15	15.63	0.53	0.42	0.32	RR1	Blazhko	
V27	09 11 53.64	-64 52 59.7	0.573229	RR0	blend	
V28	09 11 50.58	-64 51 27.8	0.2767642	16.58	16.25	15.74	16.56	16.25	15.76	0.64	0.53	0.36	RR1	Blazhko	
V29	09 12 00.53	-64 51 39.2	2.22211	15.50	14.82	13.90	15.52	14.84	13.92	0.70	0.52	0.38	BL Her		
V30	09 11 49.37	-64 51 52.6	3.25710	17.84	17.48	16.83	17.85	17.49	16.84	...	1.42	...	E	detached eclipsing binary	
V31	09 11 57.08	-64 51 29.7	...	15.25	13.39	11.35	LPV	LW1	
V32	09 11 58.71	-64 51 28.6	...	15.19	13.72	12.18	LPV	LW2	
V33	09 11 59.24	-64 52 59.2	...	15.14	13.39	11.36	LPV	LW3	
V34	09 12 01.44	-64 51 37.7	13.16	11.3	LPV	LW4	
V35	09 12 01.69	-64 50 33.3	...	15.40	13.52	11.55	LPV	LW5	
V36	09 12 02.28	-64 51 18.5	...	15.1	13.45	11.64	LPV	LW6	
V37	09 12 02.69	-64 52 01.9	...	15.1	13.7	12.1	LPV	LW7	
V38	09 12 04.34	-64 51 41.5	...	15.0	13.42	11.36	LPV	LW8	
V39	09 12 06.66	-64 52 18.2	...	15.2	13.51	11.61	LPV	LW9	
V40	09 12 08.51	-64 51 58.4	...	15.15	13.44	11.64	LPV	LW10	
V41	09 12 11.30	-64 52 42.2	...	15.3	13.47	11.62	LPV	LW11	
V42	09 12 14.47	-64 53 26.7	...	15.14	13.40	11.51	LPV	LW12	
V43	09 12 16.64	-64 52 02.9	...	15.23	13.51	11.58	LPV	LW13	
V44	09 12 18.48	-64 51 30.7	...	15.24	13.72	12.06	LPV	LW14	
V45	09 12 04.02	-64 51 54.0	13.46	LPV	LW15	
V46	09 11 50.35	-64 51 42.2	...	15.68	13.76	11.73	LPV	LW16	
V47	09 12 01.49	-64 50 49.4	...	15.33	13.77	12.13	LPV	LW17	
V48	09 12 04.85	-64 51 30.0	...	16.02	14.96	13.7	LPV	LW18	
V49	09 12 05.88	-64 52 08.1	...	15.05	13.41	11.67	LPV	LW19	
V50	09 12 24.79	-64 51 10.4	...	15.26	13.55	11.72	LPV	LW20	
V51	09 12 05.52	-64 51 31.1	2.10797	15.73	15.10	14.26	15.73	15.09	14.26	0.72	0.54	0.67	BL Her		
C52	09 11 48.52	-64 46 59.5	0.05981586	18.74	18.33	17.75	18.74	18.33	17.76	0.39	0.30	0.18	SX Phe		
C53	09 11 29.23	-64 45 23.3	0.05181968	18.68	18.32	17.80	18.68	18.32	17.80	0.24	0.22	0.13	SX Phe	poss. second period of $P = 0.04011174$	
C54	09 11 40.25	-64 53 12.8	0.441618	18.70	18.29	17.73	18.69	18.29	17.73	0.30	0.28	0.26	EB		

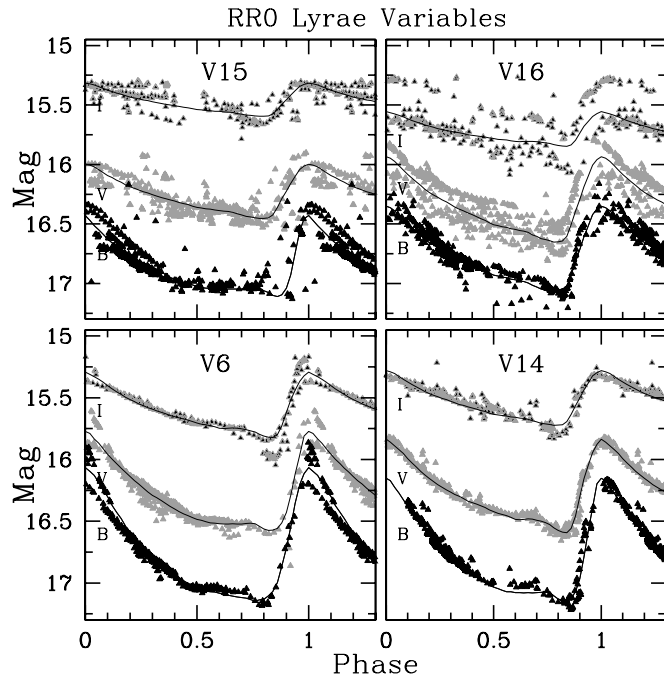


Figure 1. Presentation of the phased *BVI* light curves of fundamental-mode RR Lyrae variables in NGC 2808.

We estimate that the astrometry presented is accurate to better than $0''.1$ (see Section 2). Columns contain (1) the name of the variable as given in the 2011 update of NGC 2808 in the Clement et al. (2001) catalog, (2) the right ascension in hours, minutes, and seconds (epoch J2000), (3) the declination in degrees, arcminutes, and arcseconds, (4) the period in days, (5)–(7) the magnitude-weighted mean B , V , and I , respectively, (8)–(10) the intensity-mean B , V , and I , respectively, (11)–(13) the B -, V -, and I -amplitude, respectively, (14) the type of variable, and (15) any comments.

The following sections provide the details of the variables in NGC 2808, including the redetection of previously unknown variables.

4. RR LYRAE VARIABLES

All of the RRLs presented in Corwin et al. (2004) are recovered and found to be varying. Due to the compact nature of NGC 2808, extreme crowding and blending issues prevented us from determining magnitudes for some of the Corwin et al. (2004) variables.

The ground-based data presented here give satisfactory magnitudes and amplitudes for 4 (out of 10) stars classified by Corwin et al. (2004) as RR0 Lyrae variables, and 7 (out of 8) stars classified as RR1 (or possible RR1) stars. Five of these eight possible RR1 stars are bona fide first-overtone (FO) pulsators, whereas we could not confirm V17 as an RR1 variable. Also, the two suspect RR1 variables, V13 and V24, are found to be too bright to be RRLs belonging to the cluster, and are discussed in more detail below, in Section 8. Time-series *HST* observations would be useful to resolve the other severely blended variables. We note that the existing *HST* observations of NGC 2808 are too deep for our purposes, as the RRLs are saturated.

The light curves of the RR0 Lyrae variables are presented in Figure 1, and the RR1 stars are shown in Figure 2. The template-fitting routines from Layden (1998) and Layden & Sarajedini (2000) were used to fit the data for the determination of the

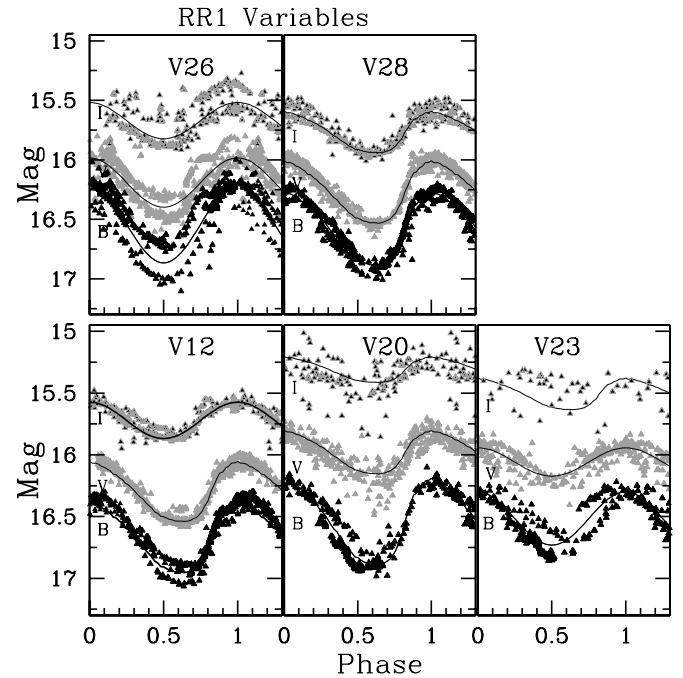


Figure 2. Phased *BVI* light curves of the first-overtone RR Lyrae variables in NGC 2808.

pulsation amplitudes. The mean magnitudes were obtained by averaging the results from the largest possible number of cycles. The difference in the magnitudes as determined from the template-fitting routines and from averaging over all observing runs is between 0.001 and 0.03 mag, depending mainly on the scatter around the template fit. Our periods for V17, V19, V21, and V25 are uncertain, as we were unable to find reasonable phased light curves for these stars from our data. Our best period for V17, $P \simeq 0.5$ days, suggests that this star is an RR0 Lyrae star or possibly a double-mode variable (RR01) instead of an RR1 as suggested by Corwin et al. (2004). The globular clusters M3 and IC 4499 are known to have RR01 variables with periods falling between 0.46 and 0.50 days (Corwin et al. 1999; Clementini et al. 2004; Clement et al. 1985; Walker 1996), and V17, V19, and V25 have periods within this general range.

The mean periods for the 11 RR0 Lyrae stars (including V17) and 5 RR1 stars are $\langle P \rangle_{RR0} = 0.56 \pm 0.01$ days and $\langle P \rangle_{RR1} = 0.30 \pm 0.02$ days, respectively. Upon the omission of V17, $\langle P \rangle_{RR0} = 0.56 \pm 0.01$ days is found, and also excluding V19, V21, and V25, gives $\langle P \rangle_{RR0} = 0.58 \pm 0.01$ days. The ratio of RR1 to total RR Lyrae stars, N_1/N_{RR} , is 0.31 (0.38 if V17 is an RR1 Lyrae star). As noted in Corwin et al. (2004), the mean periods of the RR1 and RR0 Lyrae stars are similar to those found in the typical Oosterhoff I (OoI) clusters, whereas the N_1/N_{RR} ratio is more in line with Oosterhoff II (OoII) clusters. However, Oosterhoff type I systems with similarly high RR1-type number fractions are not unprecedented (e.g., Catelan 2009, and references therein).

Except for V14, all of the RRLs show evidence of light-curve modulation, likely due to the Blazhko effect (Blazhko 1907)—a poorly understood effect that appears as a cyclic modulation of shape and amplitude of the light curve (see, e.g., Kolenberg 2011, for a recent review). Despite the relatively short time baseline of the Corwin et al. (2004) observations (two nights in 2002 December, and two nights in 2003 February), this modulation is seen in many of their light curves as well. Assuming that there are 11 RR0 Lyrae variables and 5 RR1

variables in the cluster, a lower limit of 27% and an upper limit of 91% of the RR0 variables exhibit Blazhko behavior, and 100% of the RR1s exhibit Blazhkoicity. Period doubling is an effect that would cause light-curve scatter predominantly at maximum light (e.g., Kolenberg et al. 2010; Szabó et al. 2010), and it may be that some of these stars (e.g., V6) are period doubling candidates. Although our observations span many years, the sporadic spacing and sparse consecutive sampling of our observations is not sufficient to confirm period doubling or derive Blazhko periods.

Large period-change rates can also introduce scatter in the light curves, and especially since our images span \sim 28 years, some of the light-curve scatter may be due to a rapidly changing period. However, a period change would shift the whole light curve in phase space, and not cause the variation of the shape and amplitude of the light curve, as is clearly seen in our data. We separated the light curves into different epochs of photometry and attempted to derive periods for the different subsets. However, these individual subsets were insufficient to produce period change rates that could account for the light-curve scatter—the scatter always pointed to an erratic, rather than a secular, period change. It may also be that some of the RR1 stars are in fact double-mode pulsators, although our search for secondary periods did not reveal any apparent multiple frequencies.

It is worth mentioning that faint neighbor stars may be contaminating the stellar PSF profile used to obtain our photometry. Also, inaccurate entries in the FITS headers of the archival images may contribute scatter in the light curves. We stress that we have no specific evidence for contaminated PSF fits, or of incorrect header dates, times, or filter identifications in the images employed here. But we do remain alert to the fact that PSF fitting in such crowded fields from instruments with different pixel scales and under different observing conditions is challenging, and also that the hardware and software that filled in the metadata for the images were occasionally flawed, especially in the earlier years.

The Blazhko effect has been shown to occur more often in RR0 variables with short periods ($P < 0.55$ days; Jurcsik et al. 2011; see also Preston 1964). As all the NGC 2808 RR0 Lyrae variables are OoII-type, which on average have shorter periods than OoII-type variables, a large amount of Blazhko variability in the RR0 variables is consistent with this result. As far as the RR1 stars are concerned, a large fraction of Blazhko variables is uncommon but not unprecedented (Arellano Ferro et al. 2012).

4.1. The Color–Magnitude Diagram

Figure 3 shows the positions of the RRLs in the CMDs for NGC 2808 in V versus (a) $B - I$ and (b) and (d) $V - I$. Figures 3(a) and (b) give an expanded view of the HB.

The mean apparent magnitude for the RRLs is $m_{V,RR} = 16.21 \pm 0.04$ mag, where the confidence interval is the standard error of the mean. This is in excellent agreement with the Walker (1999) estimate of $m_{V,RR} = 16.22$, obtained by comparing its red HB clump, V_{RHB} , with that of NGC 1851 and NGC 6362, both of which have a similar [Fe/H] and assuming $m_{V,RR} - V_{RHB} = -0.08 \pm 0.01$. Adopting [Fe/H] = -1.14 dex on the Carretta et al. (2009) metallicity scale ([Fe/H] = -1.00 dex on the scale of Carretta & Gratton 1997; [Fe/H] = -1.05 dex on the Kraft & Icarus 2003 scale) and using the recent recalibration of the RR Lyrae luminosity scale by Catelan & Cortés (2008), the RR Lyrae variables have an absolute magnitude of $M_V = 0.70 \pm 0.13$ mag. This leads to an RR Lyrae distance of $(m - M)_{V,RRL} =$

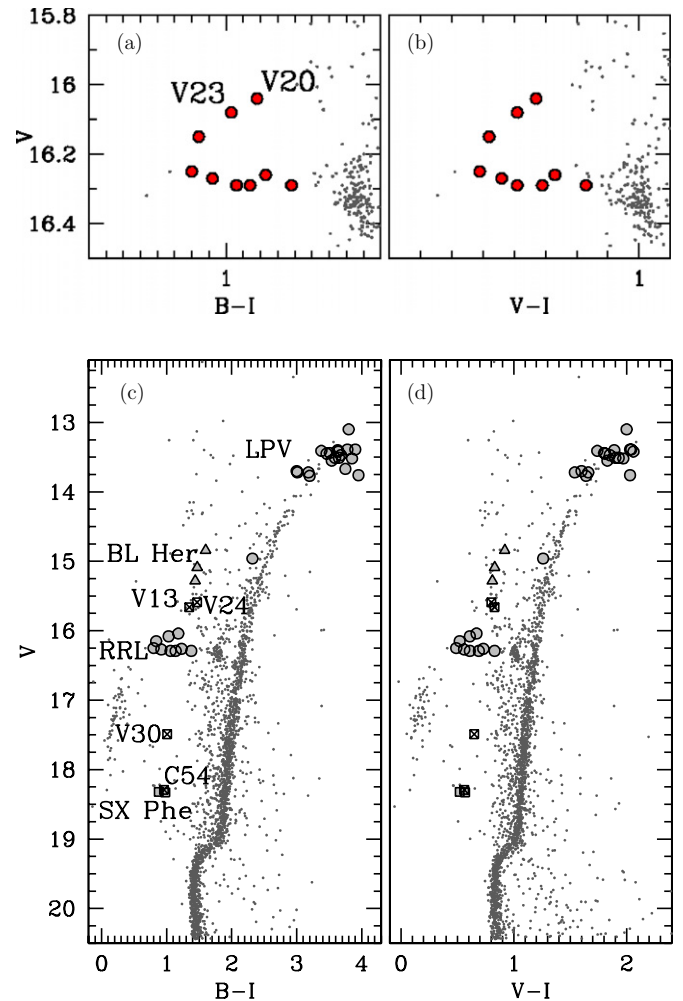
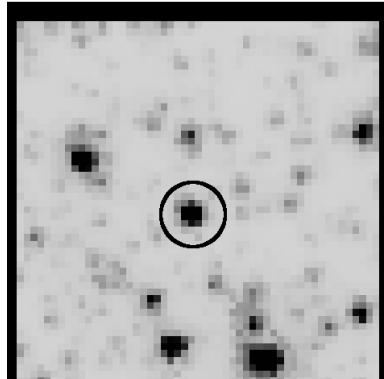


Figure 3. NGC 2808 color–magnitude diagram showing the location of the variable stars studied in this survey. The bottom two plots [c,d] show those found along the HB are clearly RR Lyrae stars, while those found to be brighter than the horizontal branch are the BL Her stars. Those variables along the giant branch are the LPVs. The SX Phoenicis stars are the faintest variables in the CMD. In the top two plots ((a), (b)) a close-up of the HB is shown.

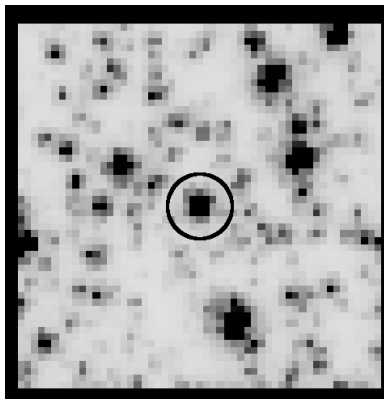
(A color version of this figure is available in the online journal.)

15.57 ± 0.13 and using $E(B - V) = 0.17$ mag (see below, Section 4.3), $(m - M)_{0,RRL} = 15.04 \pm 0.13$ mag. Similarly, using a quadratic relation between RR Lyrae absolute magnitude and metallicity from Bono et al. (2007), the RR Lyrae $M_V = 0.76 \pm 0.08$, where 0.08 is a reasonable error in the RR Lyrae absolute magnitude–[Fe/H] zero-point calibration. This leads to an $(m - M)_{V,RRL} = 15.51 \pm 0.09$ and $(m - M)_{0,RRL} = 14.98 \pm 0.09$ mag.

As seen in Figure 3, two stars are found at magnitudes brighter than the majority of the RRL stars. These are the RR1-type variables V20 and V23, and they are ~ 0.25 mag brighter than the rest of the variables. We do not believe that these stars are blended, although they both lie fairly close to the center of the cluster. Figure 4 shows thumbnails of a stacked *HST* image centered on these stars. There is no bright neighboring star within $\sim 1''.5$ of V23, and V20 is about $1''.0$ away from three relatively bright stars. Although this could contribute to slight blending, the contamination is at the level of a few percent—not much more than the uncertainty in the photometry. Because these stars have colors that overlap with the bluest part of the RR0 Lyrae region in the CMD, they may reside in the either-or



(a) V23



(b) V20

Figure 4. Stack of all available *HST* images of NGC 2808 centered on (a) V23 and (b) V20, the two brightest RR Lyrae variables in our sample. Each image is 4'0 on a side, where north is up and east is left.

region of the IS, where the transition between RR1 and RR0 takes place and where both first-overtone and fundamental-mode RRLs can be found (e.g., van Albada & Baker 1973; Caputo et al. 1978; Stellingwerf 1975; Bono et al. 1995a). It may be that these stars have evolved further from the zero-age HB and are thus more luminous. Their periods, however, are not abnormally long for RR1 variables. We also do not see any evidence for large secular period change rates, but note that finding period change rates of Blazhko stars is an especially challenging task requiring large amounts of data (Kunder et al. 2011). Sandage (1990) show that metal-rich clusters tend to exhibit a larger spread in RR Lyrae absolute magnitude (~ 0.5 mag for $[Fe/H] = -1.01$), and the spread in V we find for the RR Lyrae variables is consistent with this estimate.

Figure 5 shows the $V, (V - I)$ CMD with the blue HB, the red HB, and the RRL IS. Two Zero Age Horizontal Branches (ZAHBs) from the BaSTI α -enhanced HB tracks (Pietrinferni et al. 2004, 2006) with $[Fe/H] = -1.01$ dex are overplotted. One has a helium abundance of $Y = 0.248$ and the other has $Y = 0.30$. An apparent distance modulus of $(m - M)_V = 15.7$ mag matches the observed mean magnitude of the red HB for the normal He track. This is ~ 0.13 mag fainter than the distance modulus obtained from the RR Lyrae variables. One always expects the evolutionary mean level of the RR Lyrae stars to be different from the ZAHB, as shown by, e.g., Catelan (1992). For the metallicity of NGC 2808, the difference between the ZAHB and the average RR Lyrae magnitude is predicted to range

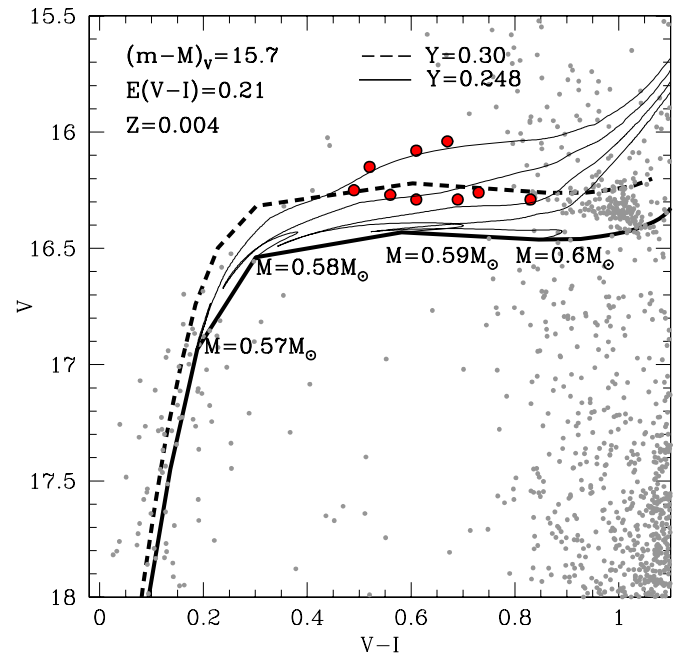


Figure 5. Optical CMD of the cluster HB compared to theoretical ZAHBs for $Y = 0.248$ (heavy solid) and $Y = 0.30$ (dashed). BaSTI HB evolutionary models are also shown for $M = 0.58 M_\odot$ and $M = 0.60 M_\odot$ HB stars with $Y = 0.248$. (A color version of this figure is available in the online journal.)

from ~ 0.18 mag (Catelan 1992) to ~ 0.1 (Gallart et al. 2005), consistent with what is found here. Therefore, a ZAHB with a primordial He abundance fits the observations well, suggesting that the majority of the RRL IS is not helium enhanced. We also show the BaSTI evolutionary tracks for $0.57 M_\odot$ and $0.60 M_\odot$ HB stars. The BaSTI tracks also indicate that most of the NGC 2808 RR Lyrae stars have a rather small mass range of $0.57\text{--}0.60 M_\odot$.

4.2. Period-Amplitude Diagram

Figure 6 shows the period–amplitude (PA) diagram for the RR Lyrae stars. Also shown in the B - and V -amplitude plane are typical lines for OoI and OoII clusters, where the fundamental-mode PA relation is derived from the M3 RRL (Cacciari et al. 2005) and the first-overtone PA relation is derived from the NGC 5286 RRL (Zorotovic et al. 2010). The Oosterhoff loci of the RRLs in the I -amplitude plane are determined using $A_V = 1.6 \times A_I$, as determined from Table 6 of Liu & Janes (1990). These relations then become

$$A_I^{RR0} = -1.64 - 13.78 \log P - 19.30 \log P^2 \quad (1)$$

$$A_I^{RR1} = -0.25 - 1.10 \log P \quad (2)$$

for fundamental-mode and first-overtone RR Lyrae stars in OoI clusters and

$$A_I^{RR0} = -0.89 - 11.46 \times \log(P) - 19.30 \times \log(P)^2 \quad (3)$$

$$A_I^{RR1} = -0.15 - 1.15 \log P \quad (4)$$

for RR Lyrae stars in OoII clusters. The period– I –amplitude relation derived for the OoII stars in M3 by Arellano Ferro et al. (2011) has a shallower slope that extends to longer periods, so the NGC 2808 RRLs fall even farther from the Arellano Ferro et al. (2011) OoII relation than to the one shown in Figure 6.

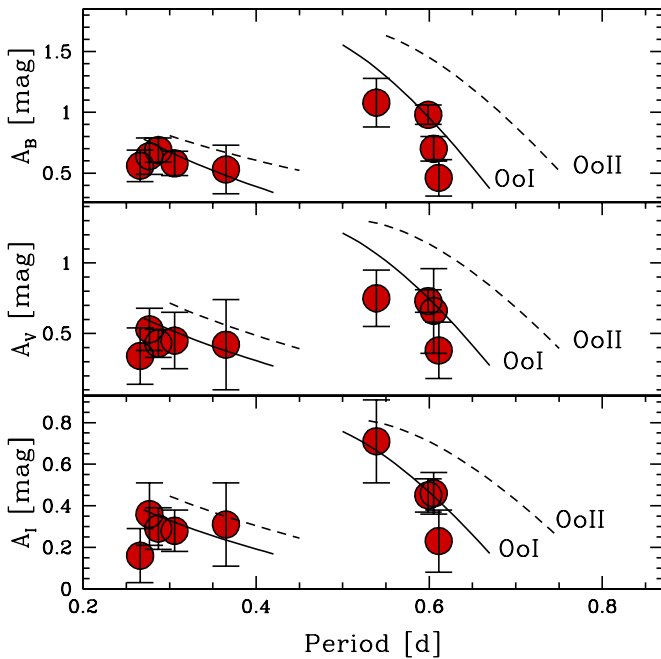


Figure 6. Position of RR Lyrae stars on the period–amplitude diagram for V (bottom), B (middle), and I (top). Solid lines are the typical lines for OoI clusters and dashed lines for OoII clusters, according to Cacciari et al. (2005) and Zorotovic et al. (2010). Because all of these stars exhibit the Blazhko effect, the error bars designate the change in amplitude from the average light curve amplitude to the maximum Blazhko amplitude.

(A color version of this figure is available in the online journal.)

The variables all occupy the area of the PA diagram where the M3 RRL as well as where other Oosterhoff I RRLs have been shown to reside (e.g., Clement & Shelton 1999). The position of a star in this diagram can be affected by the presence of the Blazhko effect (e.g., Cacciari et al. 2005), and as discussed above, almost all the RR Lyrae variables presented here show signs of this phenomenon. Because the light curves presented here have a large number of observations, it is straightforward to determine the amplitudes using the average light curves of the Blazhko stars. Nevertheless, a visual determination of the change in amplitude in each Blazhko RR0 is obtained and shown as a symmetric error bar in the figure. The change from the average light curve amplitude to the maximum Blazhko amplitude ranges from ~ 0.1 to 0.4 mag. Even when taking the amplitude variation due to the Blazhko cycle into account, the variables are all of OoI type. We note that our assumption of a symmetric Blazhko amplitude change may overestimate the lower amplitude value, as exhibited for example by the shortest-period RR Lyrae variable V23. The light curve of V23 does not seem to show amplitudes that fall to zero at some points; its error bar reaching to almost zero is an artifact of assuming symmetric error bars. Such an overestimate would not change our conclusion that all the variables are OoI-type.

4.3. RR Lyrae Reddenings

The interstellar extinction toward NGC 2808 is relatively large ($E(B - V) = 0.19$ mag; 2010 edition of Harris 1996) and differential reddening is also thought to affect the stellar colors ($\Delta E(B - V) = 0.02$; Piotto et al. 2007). Recent $E(B - V)$ values used for this cluster vary from $E(B - V) = 0.13$ (Castellani et al. 2006) to $E(B - V) = 0.23$ (Piotto et al. 2002). Here the minimum light colors of the RR0 Lyrae variables are used to investigate the reddening of NGC 2808.

Table 3
Reddening Determinations from RR Lyrae Variables in NGC 2808

Name	$(V - I)_{\min}$	$E(V - I)$
V6	0.76	0.18
V14	0.81	0.23
V15	0.84	0.26
V16	0.77	0.19

Fundamental-mode RRLs are known for their dramatic light variations, which is one of the reasons these stars are a particularly fun target to observe. At minimum light, however, RR0 Lyrae stars exhibit a much narrower temperature range (Preston 1959; Lub 1977; Fernley & Barnes 1996). This property has been used as a tool for measuring the interstellar reddening toward RRLs (Sturch 1966; Blanco 1992; Mateo et al. 1995; Kunder et al. 2010). Guldenschuh et al. (2005) showed that at minimum light (phase between 0.5 and 0.8) the color of RR Lyrae stars is $(V - I)_{0,\min} = 0.58 \pm 0.02$, and that this property is largely independent of period, amplitude, and metallicity.

The observed $V - I$ color at minimum light was calculated from both the best-fit light curve templates as well as the observed data. The values agreed to within 0.01 mag and are listed in Table 3. The number of data points in our V and I light curves that fall between a phase of 0.5–0.8 is between 35 and 200.

The average $E(V - I)$ is 0.215 ± 0.02 , or assuming a standard reddening law (e.g., Cardelli et al. 1992), $E(B - V)$ is 0.17 ± 0.02 . This is slightly smaller but still consistent with the reddening found by Bedin et al. (2000) and Walker (1999). It is also smaller than the Schlegel et al. (1998) estimate of $E(B - V) = 0.23$, but the latter reduces to 0.18—in excellent agreement with our results—after applying the correction suggested by Bonifacio et al. (2000). Our $E(B - V)$ value agrees remarkably well with the values adopted by D’Antona & Caloi (2004), Dalessandro et al. (2011), and Milone et al. (2012) when fitting isochrones to NGC 2808.

Walker (1998) showed that the blue edge of the IS in GCs appears to have a constant $B - V$ over a wide range of metallicity, with $(B - V)_{0,\text{FBE}} = 0.18 \pm 0.01$. Mackey & Gilmore (2003) find $(V - I)_{0,\text{FBE}} = 0.28 \pm 0.02$, based on two Fornax GCs. Since then Sandage (2006) found that a small dependence with $[\text{Fe}/\text{H}]$ exists at the blue fundamental edge, with $(B - V)_{0,\text{FBE}}$ varying parabolically by 0.02 mag between $[\text{Fe}/\text{H}] = -0.08$ and -2.3 dex. The bluest RRL in our admittedly small sample has $B - V = 0.31$ mag and $V - I = 0.49$ mag. This suggests an upper limit of $E(B - V) = 0.13 \pm 0.02$ we use the value of the FBE from Walker (1999) and $E(V - I) = 0.21 \pm 0.02$ or $E(B - V) = 0.17 \pm 0.02$ if we use the value of the FBE from Mackey & Gilmore (2003). The color excess values derived from both the blue edge of the IS and from the RR Lyrae minimum light colors are smaller than the generally adopted reddening value for NGC 2808 of $E(B - V) \sim 0.19$. To conclude this paragraph it is worth mentioning that the mean color of an RR Lyrae star can be different from the color of the “equivalent static star” (ESS), and the ESS color is the one that is used in such applications. Close to the blue edge of the IS, the difference between different definitions of mean colors and the color of the ESS is of the order of 0.01 mag—see Table 4 in Bono et al. (1995b). This would not change our conclusions that a slightly smaller value for $E(B - V)$ is in agreement with the results from the RRL minimum light colors.

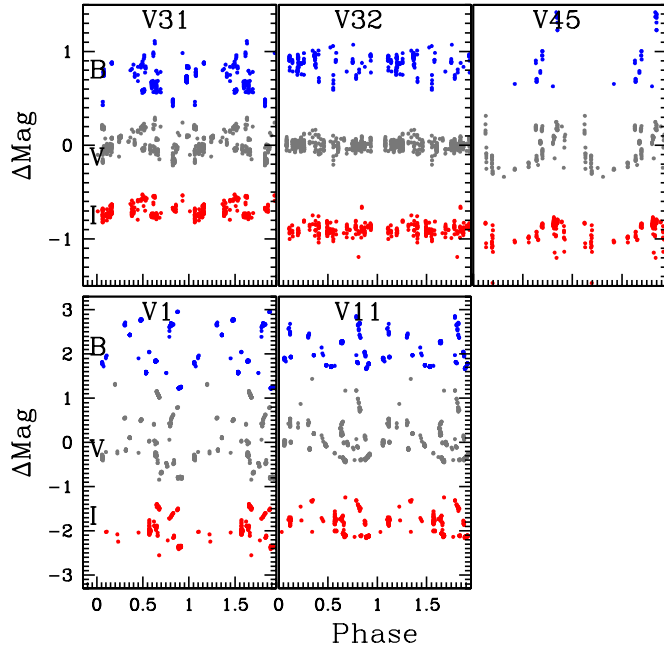


Figure 7. Presentation of the phased light curves of LPVs in NGC 2808. The *B* (top), *V* (middle), and *I* (bottom) light curves are shown in the same panel. The *B* and *I* light curves are offset by an arbitrary amount for clarity.

(A color version of this figure is available in the online journal.)

5. LONG-PERIOD VARIABLES

LPVs are radially pulsating stars on the giant branch. Especially because their pulsation is one of the several linked phenomena that control the endpoint of stellar evolution, LPV investigations provide important constraints on models of stellar evolution as well as the injection of mass into the interstellar medium (e.g., Arndt et al. 1997; Mennessier & Luri 2001; McDonald et al. 2010; Lebzelter & Wood 2011). LPVs generally show periodic variations in brightness with periods of ~ 30 up to a few thousands of days and amplitudes ranging from several tenths to approximately 10 mag in the visual. Recently Lebzelter & Wood (2011) identified 20 LPVs in NGC 2808 and claimed that a high helium abundance of $Y \sim 0.4$ is required to explain the periods of several of the LPVs. Irregularities in the light change were noted on top of the periodic variations.

The *BVI* light curves for these stars, phased with the periods obtained by Lebzelter & Wood (2011), are shown in Figure 7. Their mean magnitudes are listed in Table 2. Unfortunately, our time coverage is not suitable for a definitive investigation of the LPVs, and we do not derive periods or discuss these stars in detail here. However, as Figure 8 shows, we do note that the W/S variability index (Welch & Stetson 1993) tends to confirm that the LPVs are indeed variable. Some of the periods reported by Lebzelter & Wood (2011) failed to phase our light curves properly, but it is difficult to ascertain whether the periods are wrong or whether the scatter is merely caused by irregularities in the light curves. Especially since the three LPVs with the longest periods, as found by Lebzelter & Wood (2011), were used to infer a $Y \sim 0.4$ to explain their LPV observations, more epochs would be useful.

6. SX Phe STARS

SX Phoenicis stars (SX Phe) are of particular interest in Galactic GCs because the region of the IS that they occupy is coincident with the blue straggler region (e.g., Jeon et al.

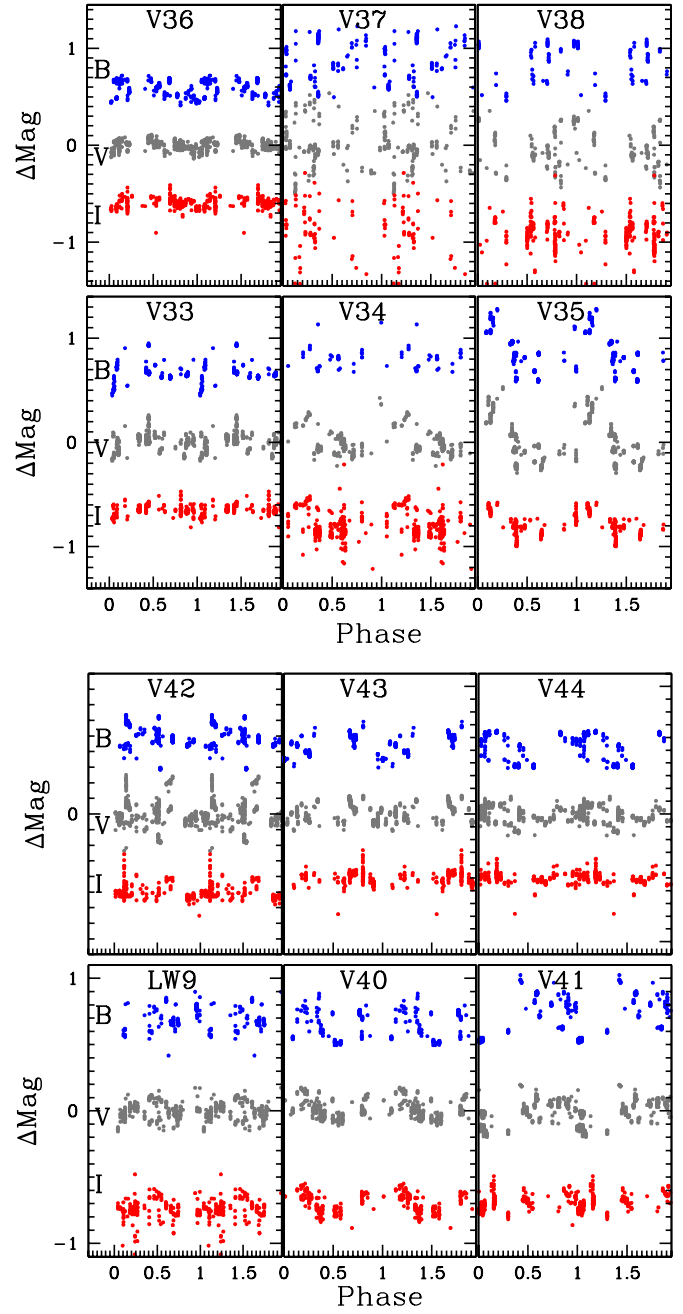


Figure 7. (Continued)

2004). This means that they have an unusual life history that is not well understood as it cannot be explained in terms of the standard single star evolution scenario. One method that may assist in the as-yet-unsolved issues of blue straggler star (BSS) formation is an analysis of their pulsation frequencies, which can provide information on the interiors of SX Phe stars (e.g., Bruntt et al. 2001; Olech et al. 2005; Cohen & Sarajedini 2012).

We have identified the first candidate SX Phe stars in NGC 2808, and their light curves are shown in Figure 9. Many SX Phe stars exhibit multiple periods and it is likely that C53 has multiple frequencies as well. The amplitude spectra of C53 for original data and after pre-whitening with subsequent frequencies is shown in Figure 10. The ratio of the periods is equal to $P_1/P_0 = 0.77$, in good agreement with observed double-mode pulsators that oscillate in the fundamental mode and the first overtone (e.g., Alcock et al. 2000; Pigulski et al.

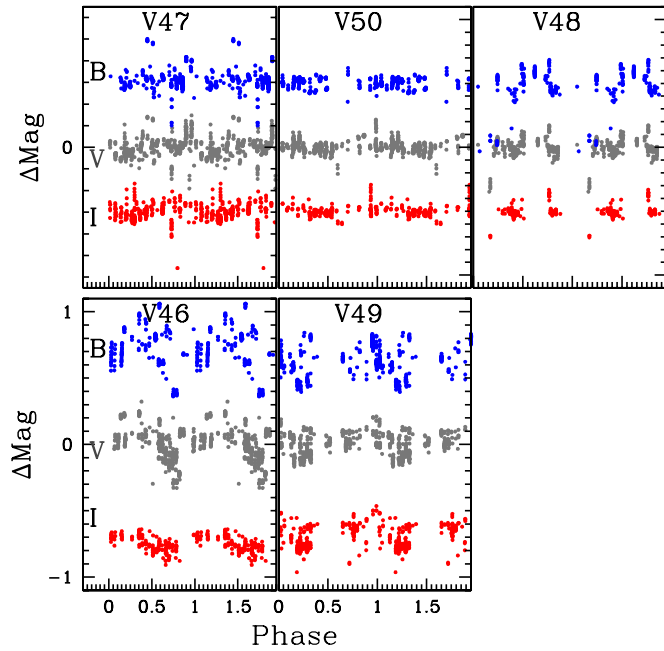


Figure 8. Welch–Stetson variability index for the LPVs, the non-variable stars, and the BL Her and RRL stars is plotted against the V magnitude. The non-variable star, V3, also has a relatively large W/S index.

(A color version of this figure is available in the online journal.)

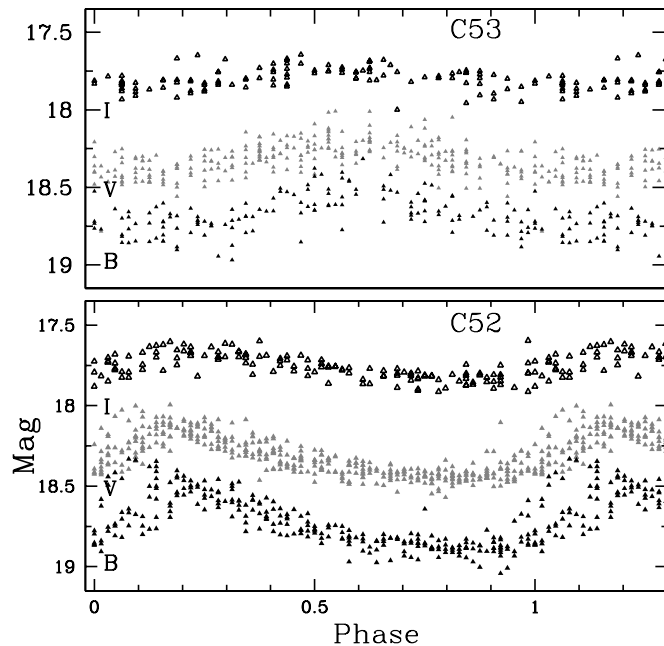


Figure 9. Phased BVI light curves of the SX Phe stars identified in NGC 2808. The primary period is used to phase the light curve of C53.

2006; McNamara et al. 2007; Garg et al. 2010). The theoretical period ratio of the first-overtone to the fundamental radial mode for SX Phe pulsators with $Z = 0.001$ ($[M/H] = -1.27$) falls in the range from 0.77 to 0.79 (Santolamazza et al. 2001), with P_1/P_0 increasing with increasing $[M/H]$. As NGC 2808 has $Z \sim 0.002$, the period ratio obtained here is well in line with the theoretical period ratio for double-mode SX Phe stars as well.

Figure 11 indicates that the periods and V -amplitudes of the SX Phe stars in NGC 2808 are consistent with those in other Galactic GCs. Figure 3 shows the positions of the two SX Phe stars in the CMD. As expected, the SX Phoenicis stars are

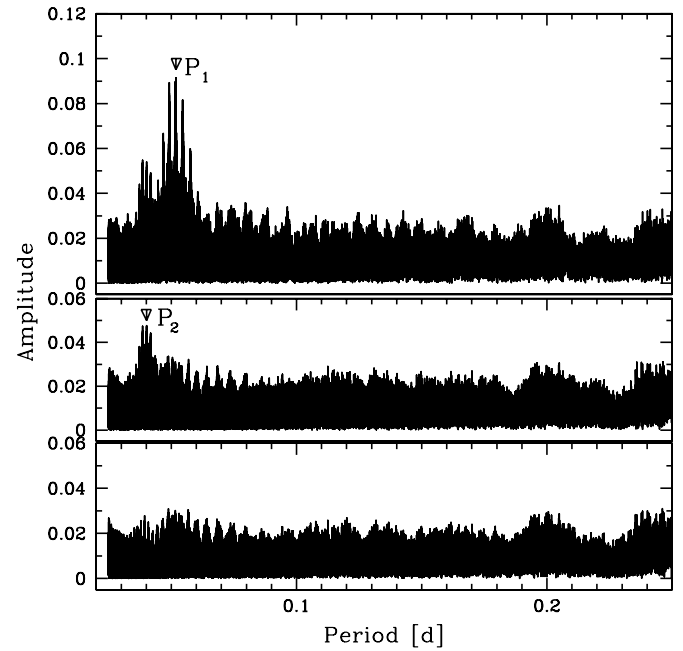


Figure 10. Fourier spectra of C53: (top) for original V -filter observations, (middle) after pre-whitening with period $P_1 = 0.05181966$ days, (bottom) after removing terms with periods $P_1 = 0.05181966$ days and $P_2 = 0.04011174$ days. The ordinate scales in all panels are the same.

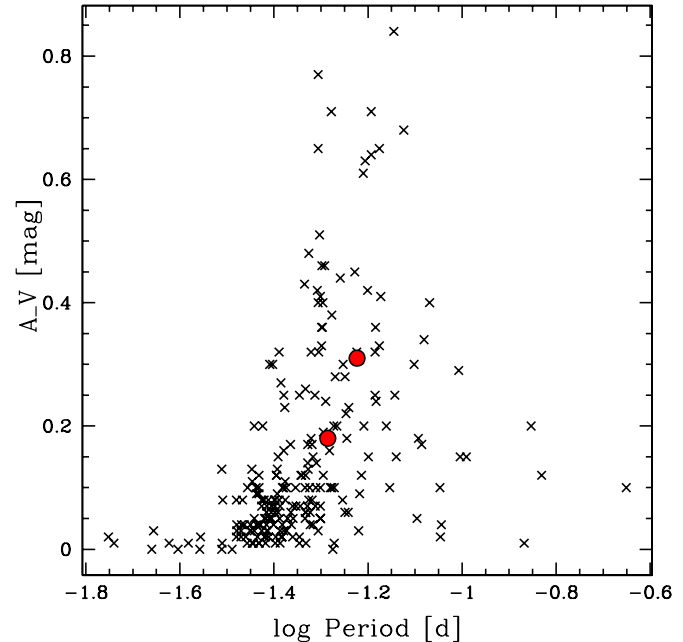


Figure 11. NGC 2808 SX Phe stars periods and V -amplitudes (filled circles) compared to the periods and amplitudes of SX Phe stars from 27 different Galactic GCs (crosses) compiled in Cohen & Sarajedini (2012).

(A color version of this figure is available in the online journal.)

located in the blue straggler region, and are brighter and bluer than the MS turnoff point.

Using 153 δ Scuti and SX Phe stars in ω Cen, M55, Carina, and Fornax, Poretti et al. (2008) derived an SX Phe period–luminosity relation

$$M_V = -1.83 - 3.65 \log P, \quad (5)$$

with a standard deviation of $\sigma = 0.18$ mag. They noted that scatter in this relation is likely caused by the existence of different pulsation modes in many SX Phe stars—which are

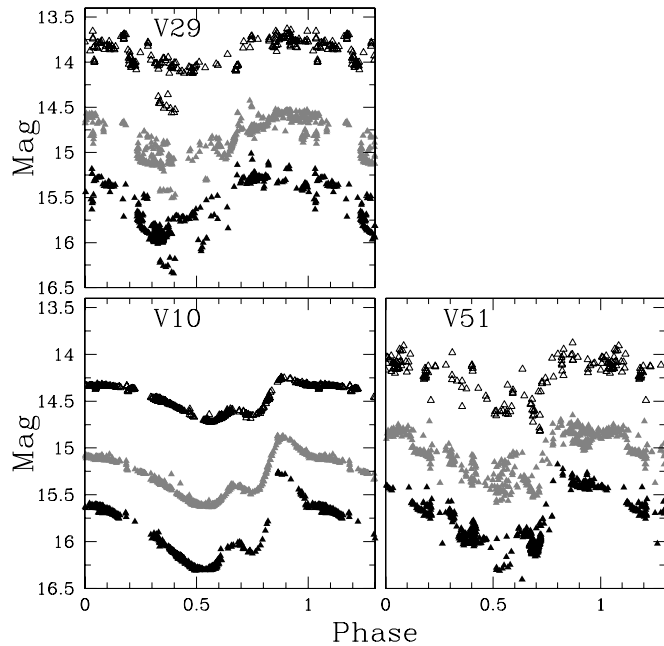


Figure 12. Phased BVI light curves of the BL Her stars in NGC 2808.

not always straightforward to identify—and the presence of subluminous SX Phe stars. Using this relation and the SX Phe stars found here, the average distance modulus to NGC 2808 is $(m - M)_{V,SXPhe} = 15.58 \pm 0.12$ mag, where the confidence interval is the standard error of the mean. Cohen & Sarajedini (2012) derived a period–luminosity relation from double-mode SX Phe stars in 27 Galactic GCs, and using their relation with our double-mode SX Phe star, C53, a distance modulus of $(m - M)_{V,SXPhe} = 15.60 \pm 0.10$ mag is found, where the error is the residual in the Cohen & Sarajedini (2012) period–luminosity fit. The two SX Phe distance estimates are in excellent agreement with each other and are also similar to the distance found using the RR Lyrae variables.

7. POPULATION II CEPHEIDS

Population II Cepheids (P2Cs) with periods between about one and eight days are usually designated BL Her variables. These stars are more luminous than RRLs and in GCs are usually found in clusters with a blue HB morphology and few RRLs (e.g., Catelan 2009). BL Her variables obey a well-defined period–luminosity relation and can be used as distance indicators (e.g., Pritzl et al. 2003; Feast et al. 2008; Matsunaga et al. 2009, 2011). We confirm V29 and V51 as BL Her variables and derive updated periods and BVI magnitudes. The light curves are shown in Figure 12. Figure 13 shows the periods and B -amplitudes of the BL Her stars in NGC 2808 compared to those in other GCs and the field. The data for the field BL Her stars come from Kwee (1968) and the data for the GCs were assembled from Pritzl et al. (2003).

Although V51 has properties indicative of a BL Her, there is more scatter in its phased light curve than for the other two presented here. The scatter may be caused by a secondary period, but BL Her stars are generally thought to be pulsating in one mode, presumably the fundamental. As shown in Schmidt et al. (2005), light curves of BL Her stars are not always very stable and that may be the case here as well. More observations would be especially helpful to investigate this star in more detail.

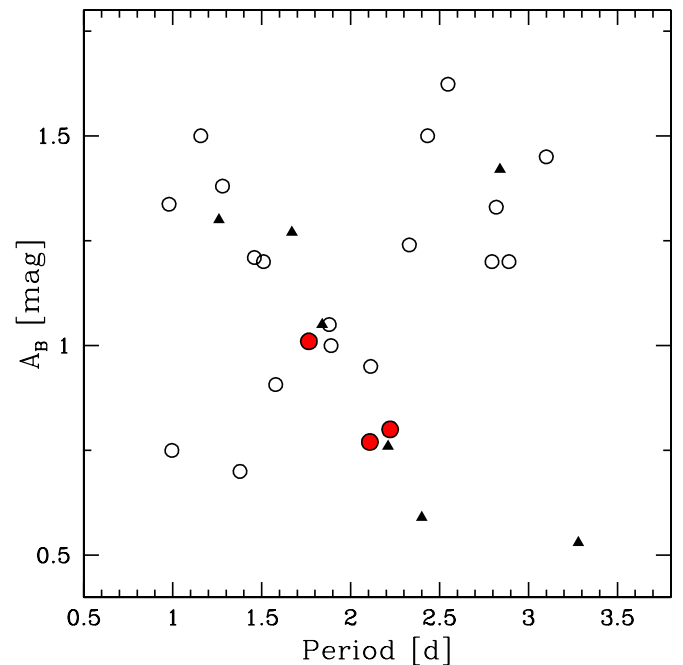


Figure 13. Period–amplitude diagram of the BL Her stars in NGC 2808. The triangles represent field BL Her stars from Kwee (1968), whereas the open circles represent GC BL Her stars from Pritzl et al. (2003).

(A color version of this figure is available in the online journal.)

Table 4
Distance Determinations from BL Her Variables in NGC 2808

Name	Period (days)	$(m - M)_{0,B}$	$(m - M)_{0,V}$	$(m - M)_{0,I}$
V10	1.76528	15.21 ± 0.10	15.11 ± 0.07	15.03 ± 0.06
V29	2.22211	14.94 ± 0.10	14.83 ± 0.07	14.68 ± 0.06
C51	2.10797	15.12 ± 0.10	15.04 ± 0.07	14.97 ± 0.06

Using the absolute magnitude relations from Pritzl et al. (2003),

$$M_V = -1.64(\pm 0.05) \log P + 0.05(\pm 0.05), \quad (6)$$

$$M_B = -1.23(\pm 0.09) \log P + 0.31(\pm 0.09), \quad (7)$$

$$M_I = -2.03(\pm 0.01) \log P - 0.36(\pm 0.03), \quad (8)$$

the distance modulus to NGC 2808 is found for all three passbands and listed in Table 4. The errors indicate the rms deviation of each relation. We adopt $E(B - V) = 0.17$ mag (see Section 4.2) and assume the canonical Galactic coefficients of selective extinction, $R_V = 3.1$, $R_B = 4.1$, and $R_I = 1.8$. The mean distance modulus is $(m - M)_{0,BLHer} = 14.99 \pm 0.06$, where 0.06 is the error in the mean (and does not take into account the rms in the absolute magnitude relations). This is slightly lower than the Harris (1996) value of $(m - M)_0 = 15.06$ (obtained using the same reddening).

Pritzl et al. (2003) calibrate these absolute magnitude relations using P2Cs from NGC 6441 and NGC 6388, clusters more metal-rich than NGC 2808. However, as shown by McNamara (1995) and Pritzl et al. (2003), there is no convincing evidence that the absolute magnitudes of these variables depend on $[Fe/H]$.

8. OTHER VARIABLES

V30–V30 was discovered by Corwin et al. (2004) and identified as an eclipsing binary star. Its light curve is shown in

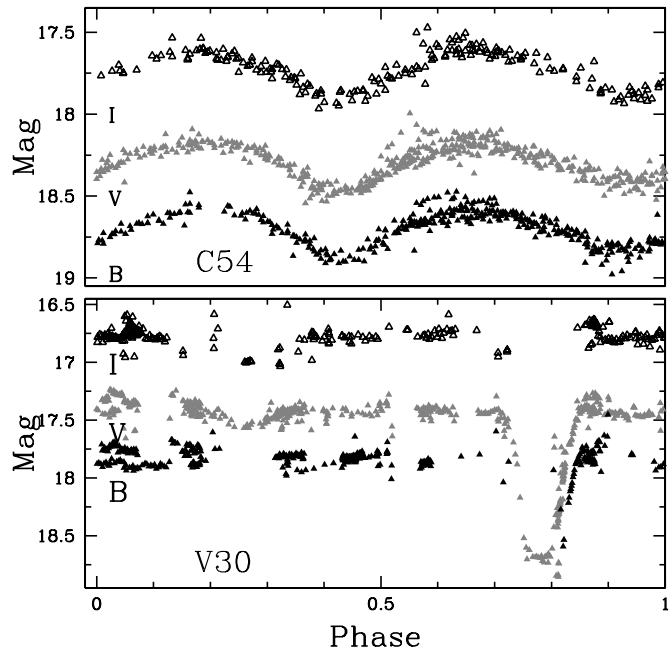


Figure 14. Phased *BVI* light curves of the eclipsing binary V30 observed in NGC 2808.

Figure 14 and is a detached eclipsing binary. Although its *V*-light curve is relatively complete, more observations, especially in the *B* and *I* passbands, would be helpful to determine the minima of the eclipse.

C54. This is a new candidate variable star, an equal-light eclipsing binary located in the blue straggler region of the CMD (see Figure 3). From a sample of 14 GCs and 20 blue straggler contact binaries, Rucinski (2000) found that their frequency of occurrence is one such system (counted as one object) per 45 ± 10 blue stragglers. As more of such systems are being identified, the frequency of contact binaries among blue stragglers can be used to constrain their currently unknown formation scenario (e.g., Mateo et al. 1990; Beccari et al. 2008).

V24. V24 was discovered by Corwin et al. (2004) and classified as an RR1. Low-amplitude variables are difficult to identify and classify (Kinman & Brown 2010), and Hoffman et al. (2009) point out that especially without color information and higher-precision photometry, the W Ursae Majoris-type variables (W UMa) and RR1 variables cannot easily be differentiated. Our photometry of V24 suggests that this star is too bright to be an RR1 variable belonging to the cluster, and therefore it may be a field W UMa or an ellipsoidal binary. Figure 15 shows that this star has a noisy, roughly sinusoidal light curve, characteristic of many W UMa stars, which are known to have light curves with shapes and average brightness levels that vary from one season to another (e.g., van't Veer 1991; Rucinski & Paczynski 2002; Borkovits et al. 2005; Hoffman et al. 2006; Pribulla & Rucinski 2006). The orbital period found is in good agreement with that of W UMa systems (Stepien et al. 2001; Rucinski 2007). However, the amplitude is decreasing when going from *B* to *I* (see Table 2), which is not a feature of W UMa stars. This star could also be a foreground RR1 star.

V24 is situated well within the 0.8 half-light radius of the cluster, so blending is always a possibility. However, if blending has brightened the star by 0.75 mag, then the blending companion must be as bright as the variable. From the *HST* thumbnail, such a large amount of blending is almost certainly

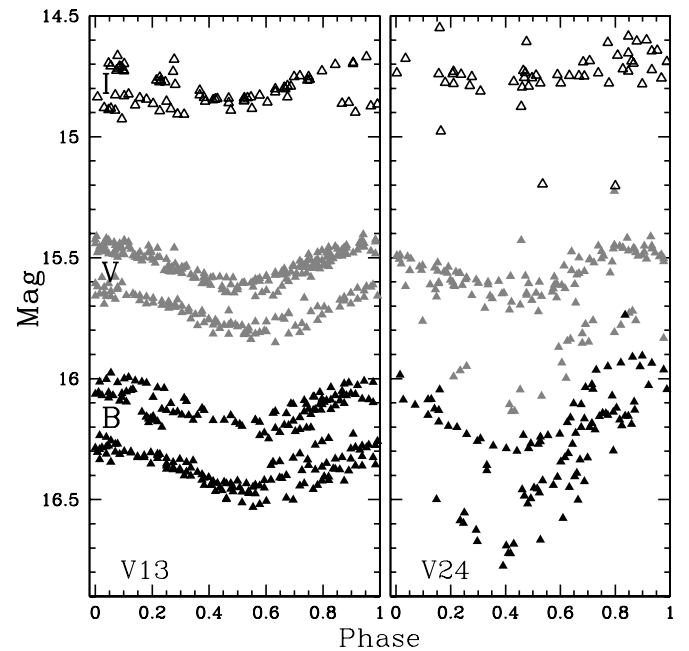


Figure 15. Phased *BVI* light curves of star V13 (left) and V24 (right) observed in NGC 2808.

not the case. We therefore still believe this star is too bright to be an RRL. On the other hand, the ratty light curve suggests that there could be some photometric problems, although we were unable to find a correlation between the magnitude offset and the seeing. The stars' χ and sharp indices are reasonable compared to the other variable stars presented here.

V13. V13 was discovered by Corwin et al. (2004) and tentatively classified as an RR1, although they noted that it might be RR2 (i.e., a second-overtone RRL) or a W UMa-type eclipsing binary. As with V24, this star is too bright to be an RRL belonging to the cluster, and may be a field W UMa, a field ellipsoidal binary, or a field RR1. Its light curve is shown in Figure 15. This star lies $\sim 7'$ from the center and is one of the most distant variables from the cluster center. As there are no stars in its immediate vicinity, it is almost certainly not blended, unless it is a real binary (separation $\ll 0.5'$, in a region where the mean separation between stars is tens of arcseconds).

8.1. Are V13 and V24 Cluster Members?

As V13 and V24 lie well within a $8'$ radius from the cluster center and have colors and magnitudes within the range of $15.4 > V > 16.5$ and $0.7 > (B - I) > 1.5$, this distance, magnitude, and color range is used to obtain a rough estimate on the likelihood of finding such field variable stars in the NGC 2808 vicinity. Our observations include ~ 140 stars with the above specified parameters, two-thirds of those stars lying closer than $2'$ from the cluster center. This is similar to the number of disk stars predicted from simulated star counts from the Besançon model (Robin et al. 2003). W UMa binaries occur in our solar neighborhood with an apparent frequency of one binary among about 500 single stars in the Galactic disk (Rucinski 2006). Therefore, although unlikely, it is tenable to find a field W UMa with a magnitude and color similar to V13 and V24. However, it is suspicious for two W UMa stars with such similar colors and magnitudes to be found in the field of NGC 2808. V13 and V24 have *V* magnitudes that are $\sim 0.5\text{--}0.8$ mag brighter than the RR Lyrae stars and colors that

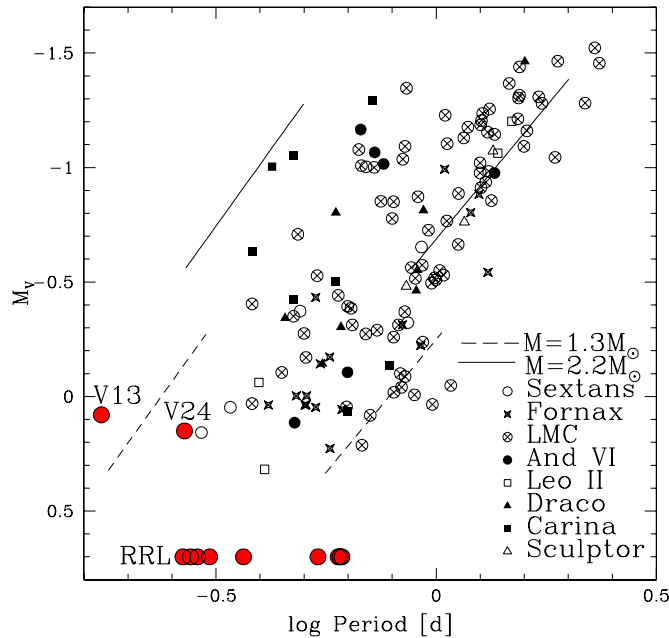


Figure 16. Observed Anomalous Cepheids in dwarf spheroidal galaxies compared with the predicted edges of the instability strip in the M_V – $\log P$ plane, from Equations (5) and (6) of Marconi et al. (2004). The dashed line indicates the predicted IS at $1.3 M_{\odot}$ and the solid line at $2.2 M_{\odot}$. To account for the occurrence of first-overtone pulsators, the blue limit is shifted by $\delta \log P = -0.13$ days. The NGC 2808 variables V13 and V24 are also shown, assuming that they are located at the distance of the cluster.

(A color version of this figure is available in the online journal.)

place them within the red and blue edges of the RR Lyrae IS (see Figure 3). These features are reminiscent of Anomalous Cepheids (ACs). In a system such as a dwarf spheroidal galaxy, ACs are ~ 0.5 mag brighter than RR Lyrae stars at periods of ~ 0.3 days, and the more luminous ACs with periods ~ 2.0 days are ~ 2.0 mag brighter than RRLs (Cox & Proffitt 1986; Bono et al. 1997b; Marconi et al. 2004).

If V13 and V24 are cluster members and assuming that the RRLs have absolute magnitudes of $M_{V,RRL} = 0.70$ (see Section 4.1), the absolute magnitudes of these stars are $M_V \sim 0.2$ mag. Figure 16, taken from Marconi et al. (2004), shows the data for well-recognized ACs in dwarf spheroidal galaxies using the distance moduli provided by various authors (see Marconi et al. 2004, for references). V13 and V24 have shorter periods and smaller amplitudes than the majority of the ACs in these galaxies, although such ACs may also be the most likely missed when looking at the comparatively great distances to the dwarf spheroidal galaxies. Chiosi et al. (1993) derive mass–period–luminosity–color relations in the BV and VI passbands for Cepheids, resulting from pulsation theory alone. From their theoretical calculations, we derive $\log T_{\text{eff}} \sim 3.73$ and $M \sim 1.5 M_{\odot}$ for V13 and $\log T_{\text{eff}} \sim 3.73$ and $M \sim 1.0 M_{\odot}$ for V24, in good agreement with those found for ACs (e.g., Bono et al. 1997b; Marconi et al. 2004). However, as clearly seen, V13 has a period that is quite different from an AC, placing this star outside the limits of the IS for its luminosity. Although ACs have been observed in many nearby Local Group dwarf galaxies, independent of their morphological type, only one or two ACs are known in Galactic GCs (V19 in NGC 5466, and possibly V7 in NGC 6341, Zinn & Dahn 1976; Matsunaga et al. 2006). We note that the light curve of V13 is similar to the AC in NGC 5466, with a brighter and a fainter sinusoidal curve varying symmetrically with each other.

V13 and V24 may also be BL Her variables, especially since BL Her stars tend to reside in GCs with extended blue tails on the HB, like NGC 2808 (e.g., Harris 1985; Sweigart & Gross 1976; Bono et al. 1997a; Wallerstein 2002; Catelan et al. 2009). However, again the periods of V13 and V24 are inconsistent with BL Her variability (~ 0.2 days versus the typical BL Her period range of 1–3 days). First-overtone BL Her stars are expected to have shorter periods and smaller amplitudes, but FO models are seen to “snuggle right up” to the fundamental pulsators (Buchler & Moskalik 1992; Moskalik & Buchler 1993; Buchler & Buchler 1994), so periods in the range of ~ 0.2 days may still be too short for FO BL Her variables. Quantitatively it is found that the blue edge for BL Her first-overtone pulsation is only ~ 100 K from the fundamental one, producing a very narrow region of FO-only pulsation (Buchler & Moskalik 1992; Buchler & Buchler 1994). This result is also supported by updated BL Her models from Di Criscienzo et al. (2008). Last, first-overtone BL Her variables are thought to be bluer than their fundamental-mode counterparts (Nemec et al. 1994), and V13 and V24 have colors similar to their fundamental-mode BL Her counterparts.

We are unable to find a secondary period for V13 and V24 from our present data, although we cannot rule out the possibility. Soszyński et al. (2008) detected the largest sample of P2Cs and ACs outside the Galaxy, finding a surprisingly large group of P2Cs with low-amplitude secondary periodicities. More observations would be desirable for a more complete frequency analysis of these stars. Spectroscopy would be useful to determine their radial velocities and therefore the probability of cluster membership. Spectra may also be able to disentangle whether these stars are varying because of an orbiting companion or because of intrinsic effects such as pulsation.

9. DISCUSSION AND CONCLUSIONS

We have presented the first calibrated BVI photometry for 11 of the 18 previously classified RR Lyrae variables in the multimodal-HB, split-MS globular cluster NGC 2808. Photometry of the other seven was hampered by the extreme crowding present within the cluster, and space-based observations are likely needed for the determination of calibrated light curves for these stars. At least two of these stars are too bright to be RR Lyrae variables, leading to a revision of the probable number of RR Lyrae stars to 16 and a specific RR Lyrae fraction of $S_{RR} = 2.8$. Here, $S_{RR} = N_{RR} \times 10^{0.4(7.5+M_V)}$, where $M_V = -9.39$ (Harris 1996, 2010 update) is the cluster’s integrated absolute magnitude in V .

We have derived pulsational parameters for all the RR Lyrae variables. Of the 16, 5 have periods consistent with first-overtone pulsators, and 11 have periods consistent with fundamental-mode pulsators, although the light-curve fit to our data for some of the RR0 stars is noisy (i.e., V17, V19, V21, V25). Our adopted periods for these stars seem to be a reasonable compromise. The mean periods of the RR0 and RR1 variables are $\langle P_0 \rangle = 0.56 \pm 0.01$ days and $\langle P_1 \rangle = 0.30 \pm 0.02$ days, respectively, and the number ratio of the RR1-type variables to the total number of the RRL-type variables is $N_1/N_{RR} = 0.3$. Using the period–amplitude diagram, the Oosterhoff type of NGC 2808 is that of an OOI cluster, which is expected considering the RR Lyrae mean periods as well as the fairly high metallicity of NGC 2808 ([Fe/H] ~ -1.14 dex; Harris 1996, 2010 edition). On the other hand, the number ratio of RR1 to total RR Lyrae stars is on the high end of typical OOI-type clusters.

The mean magnitude for the RRLs is $m_{V,RR} = 16.21 \pm 0.04$ mag, and the reddening from their minimum light colors

was determined to be $E(B - V) = 0.17 \pm 0.02$ mag, in agreement with previous studies (e.g., Walker 1999; Bedin et al. 2000). Using the recent recalibration of the RR Lyrae luminosity scale by Catelan & Cortés (2008), the RR Lyrae variables have absolute magnitudes of $M_V = 0.70 \pm 0.13$ mag. This leads to an RR Lyrae distance of $(m - M)_{V,\text{RRL}} = 15.57 \pm 0.13$ and adopting $E(B - V) = 0.17$ mag, $(m - M)_{0,\text{RRL}} = 15.04 \pm 0.13$ mag.

From the comparison of theoretical ZAHB sequences with observations, we find that most RRLs have a mass of $M = 0.57\text{--}0.60 M_\odot$ and that the RRL IS is well matched by models with standard He values ($Y = 0.248$ in this case). That the NGC 2808 RRL are not He enhanced is also supported by their derived V -amplitudes and periods. Their pulsational properties are similar to the RRL in M3, a cluster in which any helium enhancement is very likely less than 0.01 along the HB (Catelan et al. 2009). In fact, all of the RRL have OOI-type characteristics and do not show large period shifts (see Figure 6), such as are expected for RRL with high luminosities indicative of He-enrichment (Sweigart & Catelan 1998; Pritzl et al. 2002; Sollima et al. 2006; Marconi et al. 2011; Kunder et al. 2012).

Still, we are hesitant to associate the RR Lyrae stars with the red HB. This is largely because it is unclear what enhancement in the He abundance to expect for a given level of [O/Fe] depletion and [Na/Fe], [Al/Fe] enhancement. (See Catelan 2012 for a recent discussion.) For example, Marcolini et al. (2009) show that there is a wide range of possible He values for the same predicted [O/Fe] depletion level—including some very small He enhancement, of the order of ~ 0.01 , for $[\text{O}/\text{Fe}] < -0.5$ (see their Figure 16). It is therefore not impossible that the RR Lyrae stars are indeed associated with the hotter HB component of the cluster, but with a level of He enhancement that is just too small to manifest itself clearly in our data.

Except for one, all of the RR Lyrae variables studied, both the fundamental and first-overtone, show evidence of light curve modulation. This is abnormal and may be partially due to inaccuracies in our ground-based photometry and/or the Blazhko effect. The precision of our photometry is sometimes 0.05 mag, for the most crowded RR Lyrae stars, making it difficult to confirm or refute Blazhkoicity in the variables. Space-based observations, image subtraction software, and more photometry would help to shed light on which stars are Blazhko stars and which are affected by crowding/blending issues, large period change rates, double-mode pulsation, or the period doubling phenomenon. If the variables in NGC 2808 are confirmed as Blazhko stars, the unusually high Blazhko ratio would be similar to that of NGC 5024 (M53), a GC hosting one of the largest percentages of Blazhko variables, 36% and 66% of the total population of RR0 and RR1 stars in the cluster, respectively (Arellano Ferro et al. 2012). However, unlike M53, NGC 2808 is relatively metal-rich. A high percentage of Blazhko stars in a metal-rich system would be in contrast to the suggestion of a correlation between the occurrence of the Blazhko effect and metallicity.

Our observations were insufficient to discern the nature of two variable stars, V13 and V24. These two stars are ~ 0.8 mag brighter than the RR Lyrae variables, have colors that place them near the red edge of the RRL IS, and have noisy light curves. Their periods of ~ 0.2 days make it difficult to classify these stars as either ACs or BL Her stars. However, statistically it is curious to find two field W UMa variables or ellipsoidal binaries with similar colors and magnitudes to not only each other, but also to the NGC 2808 RRL and BL Her stars.

NGC 2808 has been tentatively associated with the Canis Major dwarf spheroidal galaxy. The RRL pulsational properties are somewhat unusual compared with bona fide Galactic GCs, but unlike what is typically seen in the Galaxy's dwarf satellites (e.g., Catelan 2009 and references therein), there is no evidence that NGC 2808 is an Oosterhoff-intermediate GC. The reddening and distance modulus derived in this work are similar to those previously accepted for the cluster (Harris 1996), and so the conclusions reached by Crane et al. (2003) and Forbes et al. (2004) regarding its possible association with this dwarf galaxy are not significantly affected by these new estimates. Although NGC 2808 is not particularly RR Lyrae-rich, it does harbor RR Lyrae variables, unlike the field stars located in Canis Major (Kinman et al. 2004; Mateu et al. 2009). If V13 and V24 are shown to be ACs, this would suggest an extragalactic origin for NGC 2808, as ACs are found mainly in dwarf spheroidals and are very rare, though not unprecedented, in Galactic GCs.

Two new candidate SX Phe stars and one new candidate eclipsing binary in the blue straggler region of the CMD are found in the field of NGC 2808. The SX Phe and BL Her stars have typical pulsational properties compared to other Milky Way GCs. From the three BL Her stars in NGC 2808, the distance to the cluster is $(m - M)_{V,\text{BLHer}} = 15.50 \pm 0.12$ and from the two SX Phe stars, $(m - M)_{V,\text{SXPh}} = 15.58 \pm 0.12$ is found, in good agreement with the distance determined by the RRLs.

We are grateful to Giuseppe Bono for helpful discussions regarding V13 and V24. M.C. and P.A. are supported by the Chilean Ministry for the Economy, Development, and Tourism's Programa Iniciativa Científica Milenio through grant P07-021-F, awarded to The Milky Way Millennium Nucleus; by the BASAL Center for Astrophysics and Associated Technologies (PFB-06); by Proyecto Fondecyt Regular #1110326; and by Proyecto Anillo ACT-86. This work has made use of BaSTI Web tools.

REFERENCES

- Alcaino, G. 1971, *A&A*, **15**, 360
- Alcock, C., Allsman, R. A., Alves, D. R., et al. 2000, *ApJ*, **536**, 798
- Arellano Ferro, A., Bramich, D. M., Figuera Jaimes, R., Giridhar, S., & Kuppuswamy, K. 2012, *MNRAS*, **420**, 1333
- Arellano Ferro, A., Figuera, J. R., Giridhar, S., et al. 2011, *MNRAS*, **416**, 2265
- Arndt, T. U., Fleisher, A. J., & Sedlmayr, E. 1997, *A&A*, **327**, 614
- Asano, N., & Sugimoto, D. 1968, *ApJ*, **154**, 1127
- Beccari, G., Pulone, L., Ferraro, F. R., et al. 2008, *MmSAI*, **79**, 360
- Bedin, L. R., Piotto, G., Zoccali, M., et al. 2000, *A&A*, **363**, 159
- Blanco, V. 1992, *AJ*, **104**, 734
- Blazhko, S. 1907, *AN*, **175**, 325
- Bonifacio, P., Monai, S., & Beers, T. C. 2000, *AJ*, **120**, 2065
- Bono, G., Caputo, F., & di Criscienzo, M. 2007, *A&A*, **476**, 779
- Bono, G., Caputo, F., & Marconi, M. 1995a, *AJ*, **110**, 2365
- Bono, G., Caputo, F., & Santolamazza, P. 1997a, *A&A*, **317**, 171
- Bono, G., Caputo, F., Santolamazza, P., Cassisi, S., & Piersimoni, A. 1997b, *AJ*, **113**, 2209
- Bono, G., Caputo, F., & Stellingwerf, R. F. 1995b, *ApJS*, **99**, 263
- Borkovits, T., Elkhateeb, M. M., Csizmadia, Sz., et al. 2005, *A&A*, **441**, 1087
- Bragaglia, A., Carretta, E., Gratton, R., et al. 2010, *A&A*, **519**, 60
- Bruntt, H., Frandsen, S., Gilliland, R. L., et al. 2001, *A&A*, **371**, 614
- Buchler, J. R., & Buchler, N. E. G. 1994, *A&A*, **285**, 213
- Buchler, J. R., & Moskalik, P. 1992, *ApJ*, **391**, 736
- Cacciari, C., Corwin, T. M., & Carney, B. W. 2005, *AJ*, **129**, 267
- Cáceres, C., & Catelan, M. 2008, *ApJS*, **179**, 242
- Caputo, F., Tornambé, A., & Castellani, V. 1978, *A&A*, **67**, 107
- Cardelli, J. A., Sembach, K. R., & Mathis, J. S. 1992, *AJ*, **104**, 1916
- Carney, B. W., Storm, J., & Jones, R. V. 1992, *ApJ*, **386**, 663
- Carretta, E., Bragaglia, A., Gratton, R., D'Orazi, V., & Lucatello, S. 2009, *A&A*, **508**, 695
- Carretta, E., & Gratton, R. G. 1997, *A&AS*, **121**, 95
- Castellani, V., Iannicola, G., Bono, G., et al. 2006, *A&A*, **446**, 569

- Catelan, M. 1992, *A&A*, **261**, 443
- Catelan, M. 1998, *ApJ*, **495**, L81
- Catelan, M. 2008, *MmSAI*, **79**, 388
- Catelan, M. 2009, *Ap&SS*, **320**, 261
- Catelan, M. 2012, arXiv:1211.3150
- Catelan, M., Borissova, J., Sweigart, A. V., & Spassova, N. 1998a, *ApJ*, **494**, 265
- Catelan, M., & Cortés, C. 2008, *ApJ*, **676**, L135
- Catelan, M., Sweigart, A. V., & Borissova, J. 1998b, in ASP Conf. Ser. 135, A Half Century of Stellar Pulsation Interpretations: A Tribute to Arthur N. Cox, ed. P. A. Bradley & J. A. Guzik (San Francisco, CA: ASP), 41
- Catelan, M., Grundahl, F., Sweigart, A. V., Valcarce, A. A. R., & Cortés, C. 2009, *ApJ*, **695**, 97
- Chiosi, C., Wood, P. R., & Capitanio, N. 1993, *ApJS*, **86**, 541
- Clement, C. M., & Hazen, M. L. 1989, *AJ*, **97**, 414
- Clement, C. M., Nemec, J. M., Robert, N., et al. 1985, *AJ*, **92**, 825
- Clement, C. M., & Shelton, I. 1999, *ApJ*, **515**, L85
- Clement, C. M., Muzzin, A., Dufton, Q., et al. 2001, *AJ*, **121**, 2587
- Clementini, G., Corwin, T. M., Carney, B. W., & Sumerel, A. N. 2004, *AJ*, **127**, 938
- Cohen, R. E., & Sarajedini, A. 2012, *MNRAS*, **419**, 342
- Corwin, M. T., Catelan, M., Borissova, J., & Smith, H. A. 2004, *A&A*, **421**, 667
- Corwin, T. M., Carney, B. W., & Allen, D. M. 1999, *AJ*, **117**, 1332
- Cox, A. N., & Proffitt, C. R. 1986, *LNP*, **254**, 397
- Crane, J. D., Majewski, S. R., Rocha-Pinto, H. J., et al. 2003, *ApJ*, **594**, L119
- Dalessandro, E., Salaris, M., Ferraro, F. R., et al. 2011, *MNRAS*, **410**, 694
- D'Antona, F., Bellazzini, M., Caloi, V., et al. 2005, *ApJ*, **631**, 868
- D'Antona, F., & Caloi, V. 2004, *ApJ*, **611**, 871
- De Santis, R. 2001, *MNRAS*, **326**, 397
- Di Criscienzo, M., Caputo, F., Marconi, M., & Cassisi, S. 2008, *MmSAI*, **79**, 713
- Dieball, A., Knigge, C., Zurek, D. R., Shara, M. M., & Long, K. S. 2005, *ApJ*, **625**, 156
- Feast, M. W., Laney, C. D., Kinman, T. D., van Leeuwen, F., & Whitelock, P. A. 2008, *MNRAS*, **386**, 2115
- Fernley, J. A., & Barnes, T. G. 1996, *A&A*, **312**, 957
- Forbes, D. A., Strader, J., & Broode, J. P. 2004, *AJ*, **127**, 3394
- Fourcade, C. R., & Laborde, J. R. 1966, *Atlas y Catalogo de Estrellas Variables en Cumulos Globulares al Sur de -29°, Cordoba*
- Gallart, C., Zoccali, M., & Aparicio, A. 2005, *ARA&A*, **43**, 387
- Garg, A., Cook, K. H., Nikolaev, S., et al. 2010, *AJ*, **140**, 328
- Guldenschuh, K. A., Layden, A. C., Wan, Y., et al. 2005, *PASP*, **117**, 721
- Harris, H. C. 1985, in *Cepheids: Theory and Observations*, ed. B. F. Madore (London: Cambridge Univ. Press), 232
- Harris, W. E. 1996, *AJ*, **112**, 1487
- Hoffman, D., Harrison, T., & McNamara, B. 2009, *AJ*, **138**, 466
- Hoffman, D., Harrison, T., McNamara, B. W., et al. 2006, *AJ*, **132**, 2260
- Jeon, Y.-B., Lee, M. G., Kim, S.-L., & Lee, H. 2004, *AJ*, **128**, 287
- Jurcsik, J., Szeidl, B., Clement, C., Hurta, Zs., & Lovas, M. 2011, *MNRAS*, **411**, 1763
- Kinman, T. D., & Brown, W. R. 2010, *AJ*, **139**, 2014
- Kinman, T. D., Saha, A., & Pier, J. R. 2004, *ApJ*, **605**, L25
- Kolenberg, K. 2011, in *Carnegie Observatories Astroph. Ser.*, vol. 5, ed. A. McWilliam (Pasadena, CA: The Observatories of the Carnegie Institution of Washington), 100
- Kolenberg, K., Szabó, R., Kurtz, D., et al. 2010, *ApJ*, **713**, L198
- Kraft, R. P., & Icarus, I. I. 2003, *PASP*, **115**, 143
- Kunder, A. M., Chaboyer, B., & Layden, A. 2010, *AJ*, **139**, 415
- Kunder, A. M., Salaris, M., Cassisi, S., et al. 2012, *AJ*, **145**, 25
- Kunder, A., Stetson, P. B., Catelan, M., Amigo, P., & De Propris, R. 2011, in *Carnegie Observatories Astroph. Ser.*, vol. 5, ed. A. McWilliam (Pasadena, CA: The Observatories of the Carnegie Institution of Washington), 100
- Kwee, K. K. 1968, *BAN*, **19**, 374
- Landolt, A. U. 1973, *AJ*, **78**, 959
- Landolt, A. U. 1983, *AJ*, **88**, 439
- Landolt, A. U. 1992, *AJ*, **104**, 340
- Layden, A. C. 1998, *AJ*, **115**, 193
- Layden, A. C., & Sarajedini, A. 2000, *AJ*, **119**, 1760
- Lebzelter, T., & Wood, P. R. 2011, *A&A*, **529**, 137
- Lee, Y.-W., Joo, S.-J., Han, S.-I., et al. 2005, *ApJ*, **621**, 57L
- Liu, T., & Janes, K. A. 1990, *ApJ*, **354**, 273
- Lub, J. 1977, *A&AS*, **29**, 345
- Mackey, A. D., & Gilmore, G. F. 2003, *MNRAS*, **345**, 747
- Marconi, M., Bono, G., Caputo, F., et al. 2011, *ApJ*, **738**, 111
- Marconi, M., Fiorentini, G., & Caputo, F. 2004, *A&A*, **417**, 1101
- Marcolini, A., Gibson, B. K., Karakas, A. I., & Sánchez-Blázquez, P. 2009, *MNRAS*, **395**, 719
- Mateo, M., Harris, H. C., Nemec, J., & Olszewski, E. W. 1990, *AJ*, **100**, 469
- Mateo, M., Udalski, A., Szymanski, M., et al. 1995, *AJ*, **109**, 588
- Mateu, C., Vivas, A. K., Zinn, R., Miller, L. R., & Abad, C. 2009, *AJ*, **137**, 4412
- Matsunaga, N., Feast, M. W., & Menzies, J. W. 2009, *MNRAS*, **397**, 933
- Matsunaga, N., Feast, M. W., & Soszyński, I. 2011, *MNRAS*, **413**, 223
- Matsunaga, N., Fukushi, H., Nakada, Y., et al. 2006, *MNRAS*, **370**, 1979
- McDonald, I., van Loon, J. Th., Dupree, A. K., & Boyer, M. L. *MNRAS*, **405**, 1711
- McNamara, D. H. 1995, *AJ*, **109**, 2134
- McNamara, D. H., Clementini, G., & Marconi, M. 2007, *AJ*, **133**, 2752
- Mennessier, M. O., & Luri, X. 2001, *A&A*, **380**, 198
- Milone, A., Piotto, G., Bedin, L. R., et al. 2012, *A&A*, **537**, 77
- Moskalik, P., & Buchler, J. R. 1993, *ApJ*, **406**, 190
- Nemec, J. M., Nemec, A. F. L., & Lutz, T. E. 1994, *AJ*, **108**, 222
- Olech, A., Dziembowski, W. A., Pamyatnykh, A. A., et al. 2005, *MNRAS*, **363**, 40
- Pasquini, L., Mauas, P., Käufl, H. U., & Cacciari, C. 2011, *A&A*, **531**, 35
- Pietrinferni, A., Cassisi, S., Salaris, M., & Castelli, F. 2004, *ApJ*, **612**, 168
- Pietrinferni, A., Cassisi, S., Salaris, M., & Castelli, F. 2006, *ApJ*, **642**, 797
- Pigulski, A., Kołaczkowski, Z., Ramza, T., & Narwid, A. 2006, *MmSAI*, **77**, 223
- Piotto, G., Bedin, L. R., Anderson, J., et al. 2007, *ApJ*, **661**, L53
- Piotto, G., King, I. R., Djorgovski, S. G., et al. 2002, *A&A*, **391**, 945
- Poretti, E., Clementini, G., Held, E. V., et al. 2008, *ApJ*, **685**, 947
- Preston, G. W. 1959, *ApJ*, **130**, 507
- Preston, G. W. 1964, *ARA&A*, **2**, 23
- Pribulla, T., & Rucinski, S. M. 2006, *AJ*, **131**, 2986
- Pritzl, B. J., Smith, H. A., Catelan, M., & Sweigart, A. V. 2002, *AJ*, **124**, 949
- Pritzl, B. J., Smith, H. A., Stetson, P. B., et al. 2003, *AJ*, **126**, 1381
- Robin, A. C., Reylé, C., Derrière, S., & Picaud, S. 2003, *A&A*, **409**, 523
- Rucinski, S. M. 2000, *AJ*, **120**, 319
- Rucinski, S. M. 2006, *MNRAS*, **368**, 1319
- Rucinski, S. M. 2007, *MNRAS*, **382**, 393
- Rucinski, S. M., & Paczynski, B. 2002, *IBVS*, **5321**
- Sandage, A. 1981, *ApJ*, **248**, 161
- Sandage, A. 1990, *ApJ*, **350**, 631
- Sandage, A. 1993, *AJ*, **106**, 687
- Sandage, A. 2006, *AJ*, **131**, 1750
- Sandage, A., Kadem, B., & Sandage, M. 1981, *ApJS*, **46**, 41
- Santolamazza, P., Marconi, M., Bono, G., et al. 2001, *ApJ*, **554**, 1124
- Schlegel, D. J., Finkbeiner, D. P., & Davis, M. 1998, *ApJ*, **500**, 525
- Schmidt, E. G., Johnston, D., Langan, S., & Lee, K. M. 2005, *AJ*, **129**, 2007
- Sollima, A., Borissova, J., Catelan, M., et al. 2006, *ApJ*, **640**, L43
- Soszyński, I., Udalski, A., Szymański, M. K., et al. 2008, *AcA*, **58**, 293
- Stepien, K., Schmitt, J. H. M. M., & Voges, W. 2001, *A&A*, **370**, 157
- Stellingwerf, R. F. 1975, *ApJ*, **195**, 441
- Stetson, P. B. 1979, *AJ*, **84**, 1056
- Stetson, P. B. 1987, *PASP*, **99**, 191
- Stetson, P. B. 1990, *PASP*, **102**, 932
- Stetson, P. B. 1994, *PASP*, **106**, 250
- Stetson, P. B. 2000, *PASP*, **112**, 925
- Stetson, P. B. 2005, *PASP*, **117**, 563
- Sturch, C. 1966, *ApJ*, **143**, 774
- Sweigart, A. V., & Catelan, M. 1998, *ApJ*, **501**, 63
- Sweigart, A. V., & Gross, P. G. 1976, *ApJS*, **32**, 376
- Sweigart, A. V., Renzini, A., & Tornambè, A. 1987, *ApJ*, **312**, 762
- Szabó, R., Kolláth, Z., Molnár, L., et al. 2010, *MNRAS*, **409**, 1244
- van Albada, T. S., & Baker, N. 1971, *ApJ*, **169**, 311
- van Albada, T. S., & Baker, N. 1973, *ApJ*, **185**, 477
- van't Veer, F. 1991, *A&A*, **250**, 84
- Walker, A. R. 1998, *AJ*, **116**, 220
- Walker, A. R. 1999, *AJ*, **118**, 432
- Walker, A. R., & Nemec, J. M. 1996, *AJ*, **112**, 2026
- Wallerstein, G. 2002, *PASP*, **114**, 689
- Welch, D. L., & Stetson, P. B. 1993, *AJ*, **105**, 1813
- Zinn, R., & Dahn, C. C. 1976, *AJ*, **81**, 527
- Zorotovic, M., Catelan, M., Smith, H. A., et al. 2010, *AJ*, **139**, 357